Transitions in population dynamics: equilibria to periodic cycles to aperiodic cycles

BRIAN DENNIS*†, R.A. DESHARNAIS‡, J. M. CUSHING§ and R.F. COSTANTINO¶

†Department of Fish and Wildlife Resources, University of Idaho, Moscow, ID 83844, USA; ‡Department of Biology, California State University, Los Angeles, CA 90032, USA; §Department of Mathematics, University of Arizona, Tucson, AZ 85721, USA; ¶Department of Biological Sciences, University of Rhode Island, Kingston, RI 02881, USA

Summary

1. We experimentally set adult mortality rates, μ_a, in laboratory cultures of the flour beetle *Tribolium* at values predicted by a biologically based, nonlinear mathematical model to place the cultures in regions of different asymptotic dynamics.
2. Analyses of time-series residuals indicated that the stochastic stage-structured model described the data quite well. Using the model and maximum-likelihood parameter estimates, stability boundaries and bifurcation diagrams were calculated for two genetic strains.
3. The predicted transitions in dynamics were observed in the experimental cultures. The parameter estimates placed the control and $\mu_a = 0.04$ treatments in the region of stable equilibria. As adult mortality was increased, there was a transition in the dynamics. At $\mu_a = 0.27$ and 0.50 the populations were located in the two-cycle region. With $\mu_a = 0.73$ one genetic strain was close to a two-cycle boundary while the other strain underwent another transition and was in a region of equilibrium. In the $\mu_a = 0.96$ treatment both strains were close to the boundary at which a bifurcation to aperiodicities occurs; one strain was just outside this boundary, the other just inside the boundary.
4. The rigorous statistical verification of the predicted shifts in dynamical behaviour provides convincing evidence for the relevance of nonlinear mathematics in population biology.

Key-words: nonlinear population dynamics, transitions in dynamic behaviour, *Tribolium*.

Journal of Animal Ecology (1997) **66**, 704–729

Introduction

Nonlinear demographic dynamics has focused debate about the nature of population fluctuations directly on theoretical phenomena such as stable and unstable equilibria, periodic and aperiodic cycles, and chaos. Much excitement and controversy surrounds these novel dynamic behaviours (May 1974, 1986, 1987; Strong 1986a; Berryman & Millstein 1989; Kareiva 1989; Poole 1989a,b; Bartlett 1990; Berryman 1991; Hassell, Comins & May 1991; Turchin & Taylor 1992; Turchin 1993). Indeed, the prospect of chaos in population dynamics has the attention of ecologists worldwide (Godfray & Blythe 1990; Olsen & Schaffer 1990;

Costantino & Desharnais 1991; Logan & Hain 1991; Tilman & Wedin 1991; Logan & Allen 1992; Tong & Smith 1992; Ascioti *et al.* 1993; Godfray & Grenfell 1993; Hanski *et al.* 1993; Hastings *et al.* 1993; Grasman & van Straten 1994; Renshaw 1994; Wilson *et al.* 1994; Ellner & Turchin 1995; Hanski & Korpimaki 1995; Kareiva 1995; Scheuring & Janosi 1996). Nevertheless, empirical evidence of nonlinear phenomena is scarce. There is a need for new experiments.

Our approach to rigorous testing of nonlinear population theory is to connect mathematical models with empirical data by means of statistical methods for nonlinear time series. We begin by deriving a biologically based demographic model. The mathematical analyses identify regions in parameter space corresponding to stable equilibria, periodic cycles,

*Correspondence author.

aperiodic motion around invariant loops, and chaos. The statistical analyses, based on a stochastic version of the demographic model, provide procedures for parameter estimation, hypothesis testing and model evaluation. The model, fitted to existing data, provides critical predictions for testing by means of manipulative experiments. The mathematics, biology and statistical analyses are thoroughly integrated.

In this paper, we report results and analyses of an experiment designed to test predictions of a nonlinear, stage-structured population model. The experimental system consists of laboratory populations of flour beetles (*Tribolium* sp.). The model is a system of three difference equations with nonlinear feedback terms reflecting cannibalistic interactions of the major life stages. The predictions are that striking shifts (bifurcations) in dynamical behaviour should occur, from stable point equilibria, to stable limit cycles, to aperiodic cycles, in response to changes in the rate of adult-stage mortality. In the experiment, we manipulated adult mortality directly by removing or adding adults in replicate cultures, in order to observe the resulting population dynamics under a wide range of mortality rate values. In extensive statistical analyses, we fitted the model to the experimental data and conducted a thorough evaluation of the model's predictions. A brief announcement of our work was given in Costantino *et al.* (1995); here we offer a complete description of our experiment, data and analyses. The ramifications of the study, particularly in relation to chaos theory in ecology, are discussed in detail. The results, we believe, should strongly encourage the study of nonlinear dynamics in other population systems.

Study design

MATHEMATICAL MODEL

The mathematical model links larval, pupal, and adult numbers at time $t + 1$ to the numbers in those stages at time t. The deterministic portion of the model, termed the 'skeleton' by Tong (1990), is a system of three difference equations:

$$L_{t+1} = b\, A_t \exp\left(-c_{el} L_t - c_{ea} A_t\right), \qquad \text{eqn 1}$$

$$P_{t+1} = L_t (1 - \mu_l), \qquad \text{eqn 2}$$

$$A_{t+1} = P_t \exp\left(-c_{pa} A_t\right) + A_t (1 - \mu_a) \qquad \text{eqn 3}$$

Here L_t is the number of feeding larvae (referred to as the L-stage), P_t is the number of large larvae, non-feeding larvae (prepupation), pupae and callow adults (called the P-stage), and A_t is the number of sexually mature adults (A-stage animals), at time t. The unit of time is 2 weeks and is, approximately, the average amount of time spent in the feeding larval stage under our experimental conditions. The time unit is also approximately the average amount of time spent in the P-stage. The quantity $b > 0$ is the number of larval

recruits per adult per unit of time in the absence of cannibalism. The fractions μ_l and μ_a are the larval and adult probabilities of mortality in one time unit. The exponential nonlinearities in the model account for the cannibalism of eggs by both larvae and adults and the cannibalism of pupae by adults. The fractions $\exp(-c_{el} L_t)$ and $\exp(-c_{ea} A_t)$ are the probabilities that an egg is not eaten in the presence of L_t larvae and A_t adults in one time unit. The fraction $\exp(-c_{pa} A_t)$ is the survival probability of a pupa in the presence of A_t adults during one time unit.

Some basic dynamic properties of the LPA model (equations 1–3) have been established. It has been proved that all orbits are bounded (Cushing & Yicang 1994; Kuang & Cushing 1995). Uniform persistence of the total population occurs for inherent net reproductive numbers greater than one, $R_0 = b\ \mu_l/(1 - \mu_a) > 1$, and global extinction occurs if $R_0 < 1$ (Cushing 1995). The uniqueness of a positive equilibrium for $R_0 > 1$ has been proved and its local stability near the bifurcation point at $R_0 = 1$ has been established (Cushing 1995). Some limited global equilibrium stability results have also been obtained (Cushing & Yicang 1994; Kuang & Cushing 1995).

The full model fitted to data was a stochastic model. The variability in the data was represented by multivariate noise added on a logarithmic scale:

$$L_{t+1} = b\, A_t \exp(-c_{el} L_t - c_{ea} A_t + E_{1t}), \qquad \text{eqn 4}$$

$$P_{t+1} = L_t (1 - \mu_l) \exp(E_{2t}), \qquad \text{eqn 5}$$

$$A_{t+1} = [P_t \exp(-c_{pa} A_t) + A_t (1 - \mu_a)] \exp(E_{3t}) \qquad \text{eqn 6}$$

Here E_{1t}, E_{2t}, and E_{3t} are random noise variables assumed to have a joint multivariate normal distribution with a mean vector of zeros and a variance–covariance matrix denoted by Σ. The noise variables represent the unpredictable departures of the observations from the skeleton (equations 1–3) due to environmental and other causes. Additive noise on the logarithmic scale is a model of stochastic forces which are manifested at all levels of population abundance (see Dennis *et al.* 1995); such stochastic forces are frequently termed environmental variability. The type of stochasticity known as demographic variability (variation in birth and death events among individuals, evident only at very low abundances) was not explicitly included in the model. The noise variables were assumed correlated with each other within a time unit (as quantified by the elements in the matrix Σ) but uncorrelated through time. These stochastic modelling assumptions were evaluated with time-series diagnostic methods (see Statistical methods).

Note that the log-scale noise can produce a value of P_{t+1} that is greater than L_t. For the P-stage recruits to exceed the supply of potential recruits in the L-stage seems, at first glance, to be unrealistic. In fact, such an event is quite possible in real cultures. Stochastic variation in developmental rates allows some eggs present at time t and some small larvae present

at time $t-1$ to be categorized as P-stage individuals at time $t+1$. The noise is a realistic model of the inevitable departures by some population members from the rigid 2-week stage passage times assumed in the deterministic model. Note also that a term for P-stage mortality from causes other than cannibalism is not included. We have found that including the term in statistical estimation procedures results in vanishingly small parameter estimates of negligible consequence to the population dynamics and have therefore omitted the term from the model.

The nonlinear map represented by the model skeleton is preserved in the stochastic model on the logarithmic scale. The conditional expected values of $\ln L_{t+1}$, $\ln P_{t+1}$, and $\ln A_{t+1}$ given values of L_t, P_t, and A_t are:

$$E(\ln L_{t+1} \mid L_t = l_t, P_t = p_t, A_t = a_t) =$$

$$\ln[b\, a_t \exp(-c_{el}\, l_t - c_{ea}\, a_t)], \quad \text{eqn 7}$$

$$E(\ln P_{t+1} \mid L_t = l_t, P_t = p_t, A_t = a_t) =$$

$$\ln[l_t\,(1-\mu_l)], \quad \text{eqn 8}$$

$$E(\ln A_{t+1} \mid L_t = l_t, P_t = p_t, A_t =$$

$$a_t) = \ln[p_t \exp(-c_{pa}\, a_t) + a_t\,(1-\mu_a)]. \quad \text{eqn 9}$$

Thus, the one-step conditional expected values retain the essential dynamical properties of the deterministic portion. Because the noise is additive on the logarithmic scale, departures of observed values of $\ln L_{t+1}$, $\ln P_{t+1}$, and $\ln A_{t+1}$ from their one-step expected values (equations 7–9) constituted the 'residuals' used for evaluating the fit of the model to data (see Statistical methods).

The stochastic model provided an explicit likelihood function for connecting data with model parameters. The likelihood function was the basis for most of the statistical analyses we performed, including point estimation and confidence intervals for parameters. The likelihood function for one population is a product of probability density functions (PDFs) for multivariate normal distributions:

$$L(\theta, \Sigma) = \prod_{t=0}^{q-1} p(w_{t+1} \mid w_t). \quad \text{eqn 10}$$

Here $w_t = [\ln l_t, \ln p_t, \ln a_t]'$ is a vector of observed stage abundances at time t, $t = 0, 1, 2, \ldots, q$ and $\theta = [b, cel, cea, cpa, \mu_l, \mu_a]'$ is a vector of unknown parameters in the model skeleton (equations 1–3). The PDF $p(w_{t+1} \mid w_t)$ represents the relative chance of the observation w_{t+1} occurring, given the stage abundances observed at time t. It is a multivariate normal PDF with a mean vector given by the one-step conditional expected values (equations 7–9) and variance-covariance matrix Σ. Most actual calculations were performed with the log-likelihood,

$$\ln L(\theta, \Sigma) = \prod_{t=0}^{q-1} \ln p(w_{t+1} \mid w_t). \quad \text{eqn 11}$$

The log-likelihood used for a complete data set representing multiple populations was the sum of the log-likelihoods for individual populations.

In a previous study (Dennis *et al.* 1995), we used the log-likelihood function (equation 11) to fit the model to an existing data set. Maximum likelihood (ML) estimates of model parameters were calculated by Dennis *et al.* (1995) for flour beetle data described by Desharnais & Costantino (1980). The ML estimates corresponded to a region of stable two-cycles for the model skeleton (Fig. 1, solid circle).

Intriguing predictions emerged from the analyses. The top portion of Fig. 1 portrays a slice of parameter space in which all parameters besides c_{pa} and μ_a have been held constant at their ML values. Shifts in dynamical behaviour should result if the adult death rate, μ_a, were increased through a range of values starting near zero and ending near one. The dashed line in Fig. 1 at the level of the ML estimate of c_{pa} shows which stability boundaries would be crossed by increasing μ_a, and a bifurcation diagram for the L-stage (Fig. 1, bottom) depicts the corresponding attractors. A population with a very low value of μ_a should display a stable equilibrium. The stable equilibrium should bifurcate to a stable two-cycle when μ_a is increased to low/intermediate values. The two-cycle should display a reverse bifurcation to a stable equilibrium when μ_a is increased to high/intermediate values. Finally, at very high values of μ_a, the stable equilibrium bifurcates to a stable, closed loop (invariant loop) in phase space: the stage abundances eventually follow points around the loop. For most of the μ_a values in the invariant loop region, the trajectories around the loop are aperiodic, that is, the stage abundances never return exactly to the same point on the loop. The resulting aperiodic fluctuations are chaos-like, although they do not constitute true 'chaos' under the usual mathematical definition. (The definition of chaos involves 'sensitivity to initial conditions' as indicated when the 'Lyapunov exponent' is greater than zero. An invariant loop has a Lyapunov exponent equal to zero and represents a possible route to chaos; see Discussion.)

EXPERIMENTAL PROTOCOL

To test these predictions of transitions in attractors as the adult death rate changes, we experimentally manipulated adult mortality rates to place cultures of the flour beetle *Tribolium castaneum* (Herbst) in regions of different asymptotic dynamics: $\mu_a = 0.04$, 0.27, 0.50, 0.73 and 0.96 (Fig. 1, open circles and arrows). There were also control cultures which were not manipulated. Unfortunately, the sensitive strain of the Fig. 1 data is no longer available, and so we performed the experiment using two other genetic
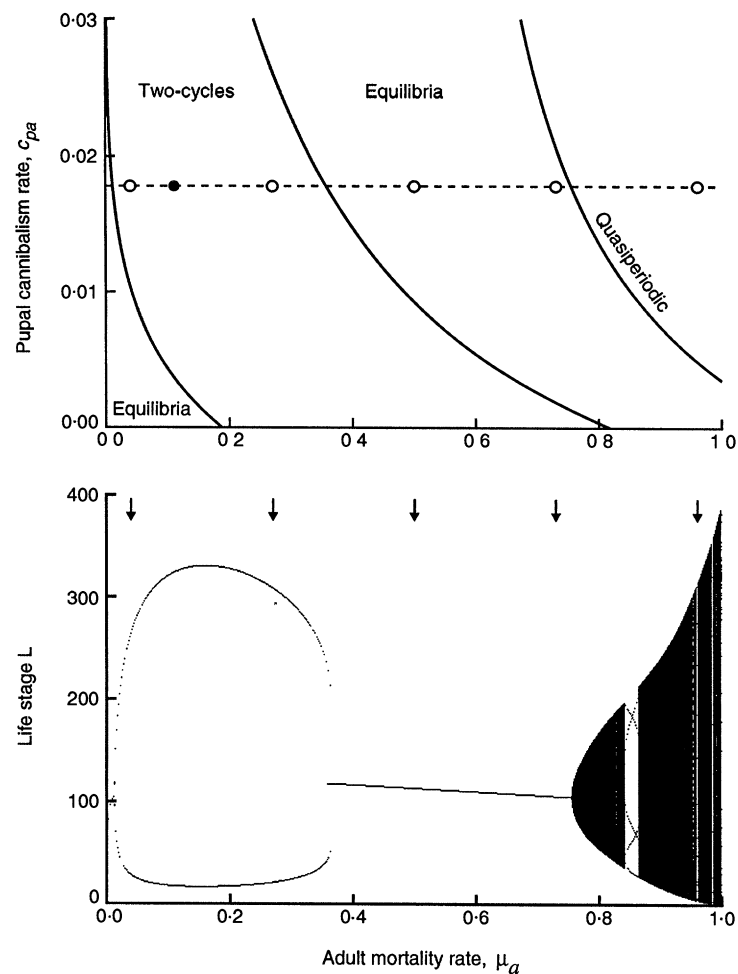
Fig. 1. Stability boundaries (top) and bifurcation diagram (bottom) show dynamical behaviours of the LPA model (equations 1–3) for different values of parameters μ_a and c_{pa}. Other parameters are fixed at the maximum likelihood estimates calculated for the sensitive genetic strain. ●, maximum likelihood estimates for μ_a and c_{pa}. ○ and ↓, predictions resulting from proposed experimental values of adult mortality rate.

strains, *RR* and *SS*. Twenty-four cultures of each strain were started with 100 young adults, five pupae and 250 small larvae. Each population was contained in a half-pint (237 mL) milk bottle with 20 g of standard media and kept in a dark incubator at 32°C. Every 2 weeks the L-, P-, and A-stages were censused and returned to fresh media. Dead adults were censused and removed. This procedure was continued for 36 weeks. At week 12, four populations of each genetic strain were randomly assigned to each of the six treatments, and the imposition of adult mortalities commenced. Adult mortality was manipulated by removing or adding adults at the time of a census to make the total number of adults that died during the interval consistent with the treatment value of adult mortality. For example, suppose there were 50 adults (A-stage individuals) counted at time t, and the target mortality was $\mu_a = 0\cdot5$. At time $t + 1$, if 20 dead adults were counted, then five living adults would be removed (bringing the total dead to $25 = \mu_a \times 50$). If instead 30 dead adults were counted at time $t + 1$, then five living adults would be added to the culture. In this

fashion, the parameter μ_a was rigorously controlled. To counter the possibility of genetic changes in life-history characteristics, beginning at week 12 and continuing every month thereafter, the adults returned to the populations after the census were obtained from separate stock cultures maintained under standard laboratory conditions.

STATISTICAL METHODS

The model was fitted separately to the *RR* and *SS* data sets. Each data set was divided in half: two populations from each treatment (including control) were picked at random and assigned to a data set used for parameter estimation. The remaining 12 populations were withheld for model evaluation.

The log-likelihood function (equation 11) was adjusted to accommodate the experimental design. Time series from the 12 'estimation' populations were combined into one log-likelihood. Each time-step for each population, representing a transition from w_t to w_{t+1}, contributed a 'ln $p(w_{t+1} \mid w_t)$ term' to the log-

likelihood. For the experimentally manipulated populations, the value of μ_a in the term $\ln p(\mathbf{w}_{t+1} | \mathbf{w}_t)$ was fixed at the corresponding experimental value (0·04, 0·27, 0·50, 0·73, or 0·96). The value of μ_a in the control populations was estimated directly from the census counts of adults at time t and dead adults at time $t + 1$ (product-binomial likelihood). The resulting estimate of μ_a was included in the time series log-likelihood as a fixed constant. The control populations and experimental populations were given different variance–covariance matrices (Σ_C and Σ_T) in the log-likelihood; we expected that the experimental treatments would alter the variability of the adult stage due to the manipulation of adult numbers.

The starting point ($t = 0$) for each time series was week 12, and each series used in the analyses lasted 24 weeks and contained 12 one-step transitions ($t = q = 12$). Although 12 observations would not normally constitute an adequate sample size for time series analysis, in our experiment all 12 populations from the 'estimation' half of the data were used to estimate a common set of parameters. The effective sample size was therefore $12 \times 12 = 144$ transitions in the log-likelihood function.

The log-likelihood function was maximized numerically using the Nelder–Mead simplex algorithm (Press *et al.* 1992). A total of 17 unknown parameters were included in the log-likelihood: b, c_{el}, c_{ea}, c_{pa}, μ_l, and six parameters each in Σ_C and Σ_T. The calculations were numerically well-behaved, and repeated maximizations from many different starting points converged to the same ML parameter values.

Confidence intervals were calculated for each unknown parameter from the skeleton (equations 1–3) using the profile likelihood method. The parameter was fixed at a value, and then the log-likelihood was maximized with respect to the remaining parameters. The process was repeated for a range of fixed values of the parameter in question. The set of such values for which the likelihood ratio test statistic (–2 ln[maximized likelihood with parameter fixed/full maximized likelihood]) was less than 3·843 (95th percentile of a chi-squared distribution with 1 d.f.) was taken as an approximate 95% confidence interval for the parameter. Dennis *et al.* (1995) provide additional details about profile likelihood methods for the flour beetle model.

Residuals and prediction errors were calculated to assess the fit and predictions of the model. Residuals were calculated on the logarithmic scale, for each state variable in each population in the 'estimation' data, by substituting the ML estimates in the conditional expected values (equations 7–9). Departures of the log-state variable from the estimated conditional expected values constituted the residuals. Prediction errors were calculated similarly, but with the 'validation' data set used instead of the 'estimation' data. Residuals and prediction errors were subjected to various diagnostic tests for autocorrelation and normality described by Dennis *et al.* (1995).

Results

POPULATIONS IN PARAMETER SPACE

ML parameter estimates for the two strains were for the most part similar (Table 1). The values of the parameter b in the *RR* and *SS* strains were consistently less than the value reported for the sensitive strain ($b = 11·7$; Dennis *et al.* 1995) on which Fig. 1 was based. All the ML estimates of the 'skeleton' parameters (b, c_{el}, c_{ea}, c_{pa}, μ_l, μ_a) have biologically reasonable values. The covariances in the variance–covariance matrices were small: the absolute values of the correlations did not exceed 0·50.

The resulting stability regions for the *RR* and *SS* strains, plotted on the c_{pa}–μ_a plane in parameter space in Figs 2 and 3, respectively, were qualitatively similar to the regions depicted for the sensitive strain in Fig. 1. The main quantitative difference between the *RR* and *SS* regions in Figs 2 and 3 and the sensitive regions in Fig. 1 is that the zones of various dynamic behaviours in the former are pushed further to the right and occur at higher values of μ_a. The lowered value of b in the *RR* and *SS* experiments produced a stabilizing effect of sorts and in particular made the aperiodic region harder to attain.

Nonetheless, the *SS* strain for the $\mu_a = 0·96$ treatment was placed by the ML estimates within the region of aperiodic fluctuations (Fig. 3). The $\mu_a = 0·96$ treatment for the *RR* strain was just outside the aperiodic region, in a region of stable point equilibria (Fig. 2). Simulations have shown that the transient approach to equilibrium for the *RR* treatment at $\mu_a = 0·96$ is extremely long and aperiodic (see Discussion), so the dynamical behaviour of the *RR* populations at $\mu_a = 0·96$ closely resembles invariant loop behaviour.

The other experimental treatments were located by the ML estimates among the different zones of dynamic behaviour (Figs 2 and 3). The control populations for both strains (extreme left points; Figs 2 and 3) were in regions in which the attractors were stable point equilibria. The $\mu_a = 0·04$ treatments for both strains were also in the stable equilibria regions. The $\mu_a = 0·27$ and $\mu_a = 0·50$ treatments were in regions where stable two-cycles govern long-range behaviour. For the *SS* strain, the $\mu_a = 0·73$ treatment populations were in a region of stable point equilibria. The $\mu_a = 0·73$ treatment for the *RR* strain was also in the stable point equilibria region, but was close to the two-cycle boundary. Overall, the transitions in dynamic behaviour in the experimental cultures (Figs 2 and 3), as classified by ML parameter estimates, were highly consistent with the transitions predicted by the earlier modelling study (Fig. 1).

OVERVIEW OF TRANSITIONS IN DYNAMIC BEHAVIOUR

The ML parameter estimates thus place the treatments in regions of different dynamic behaviours. Do the

Table 1. Maximum likelihood parameter estimates for the *RR* and *SS* genetic strains. The 95% confidence intervals (parentheses) for the parameters b, μ_l, c_{ea}, c_{el}, and c_{pa} were calculated from profile likelihoods. The estimates (and 95% confidence intervals) for μ_a were calculated directly from the numbers of dead adults observed in the control cultures. Correlations are listed in parentheses below the main diagonals of the symmetric variance–covariance matrices for control (Σ_C) and treatment (Σ_T) replicates

Parameter	*RR* strain	*SS* strain
b	7·876 (5·8, 10·7)	7·483 (5·4, 10·3)
μ_a	0·004210 (0·0032, 0·0052)	0·003620 (0·0027, 0·0045)
μ_l	0·1613 (0·10, 0·22)	0·2670 (0·21, 0·32)
c_{ea}	0·01114 (0·010, 0·012)	0·009170 (0·0081, 0·010)
c_{el}	0·01385 (0·012, 0·015)	0·01200 (0·011, 0·013)
c_{pa}	0·004348 (0·0039, 0·0048)	0·004139 (0·0037, 0·0046)

$$\Sigma_C = \begin{bmatrix} 0·5670 & -0·1452 & 0·002469 \\ (-0·49) & 0·1573 & 0·001549 \\ (0·28) & (0·31) & 0·0001541 \end{bmatrix} \qquad \begin{bmatrix} 0·08044 & 0·02820 & 0·004317 \\ (0·08) & 0·1593 & 0·003409 \\ (0·11) & (0·19) & 0·001986 \end{bmatrix}$$

$$\Sigma_T = \begin{bmatrix} 0·8280 & -0·08448 & -0·002971 \\ (-0·22) & 0·1749 & -0·02020 \\ (-0·02) & (-0·33) & 0·02057 \end{bmatrix} \qquad \begin{bmatrix} 0·8673 & 0·01366 & -0·004042 \\ (0·03) & 0·2221 & 0·01012 \\ (-0·04) & (0·21) & 0·01087 \end{bmatrix}$$
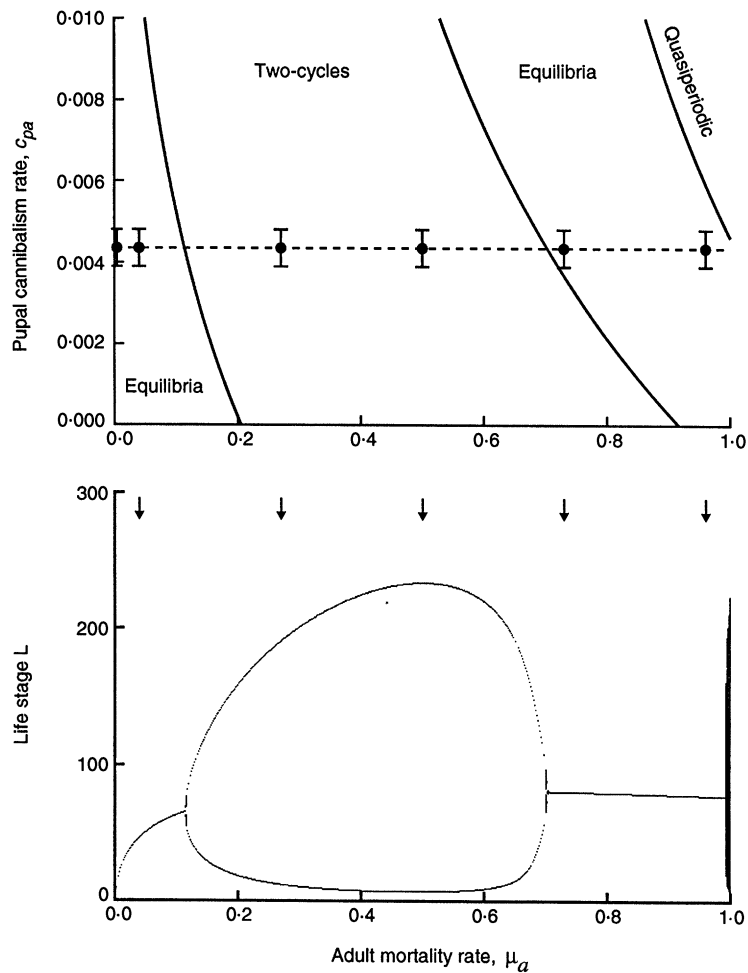

Fig. 2. Stability boundaries and bifurcation diagram for the *RR* genetic strain. ↓, experimental values of adult mortality rate. ● and bars, maximum likelihood estimates and 95% confidence intervals for locations of experimental cultures.
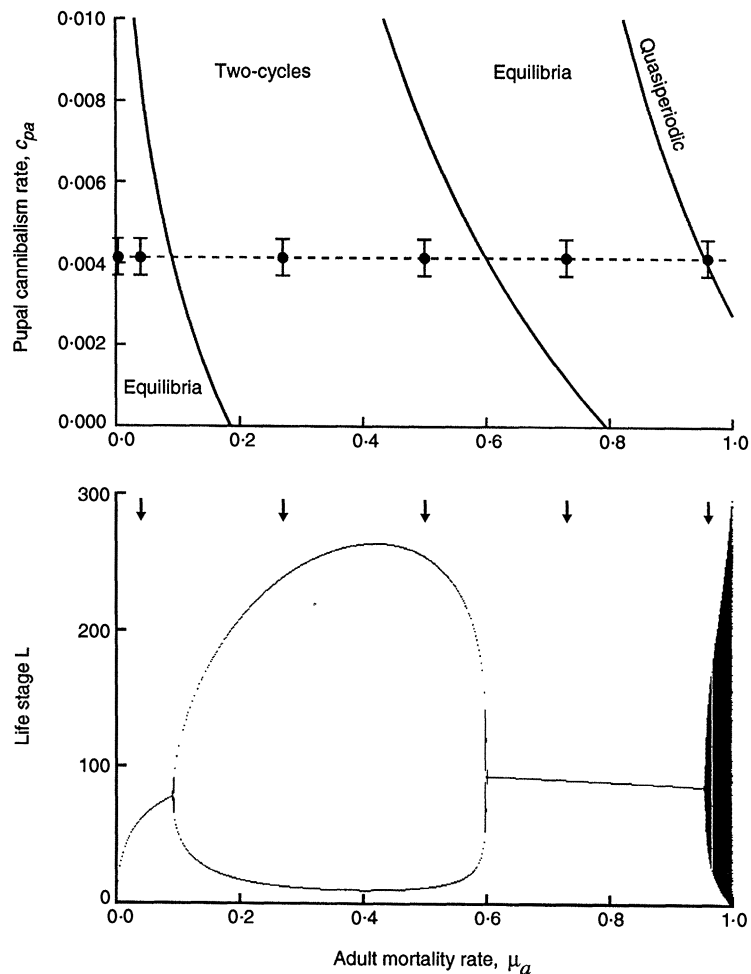
populations indeed display the predicted dynamic behaviours? In Figs 4 and 5, all the data are plotted, including the initial 12 weeks collected before the com-

mencement of the adult replacements and the adult mortality treatments. The differences in dynamic behaviours among treatments, and the resemblances

Fig. 3. Stability boundaries and bifurcation diagram for the *SS* genetic strain. Symbols as in Fig. 2.

of the treatments to the dynamic behaviours predicted by the model, are striking. Both qualitatively and quantitatively, transitions in dynamics occurred among the populations, of a nature predictable by a nonlinear mathematical model.

MODEL GOODNESS-OF-FIT

The model fitted the experimental data well. Tables 2 and 3 list results from analyses of the residuals for the *RR* and *SS* strains, respectively. The residuals, it will be recalled, were obtained from the halves of the *RR* or *SS* data sets designated for parameter estimation. The residuals are the estimated outcomes of the noise variables E_{it} in the model (equations 4–6) and should display approximately the statistical properties of the noise variables. Each individual time series of residuals, representing one state variable (L_t, P_t or A_t) from one population, was tested separately for departure from normality and autocorrelation (first- and second-order). Significant first-order autocorrelation was detected in just one (3%) of the 36 *RR* residual time series (Table 2) and in none of the *SS* series (Table 3). Significant second-order autocorrelation was detected in just two (6%) of the *RR* series and two of the *SS* series. Departure from a normal distribution was detected in 12 (33%) of the *RR* series and six (17%) of the *SS* series. Normality departures can be traced to a small number of outliers; most of the observations in each series were well described by a normal distribution. These results compare favourably with the same analyses reported by Dennis *et al.* (1995, Table 2) for 12 series of the sensitive strain (no first-order autocorrelated series (0%), two second-order autocorrelated (17%), three non-normal series (25%)).

PREDICTION ERROR

Model predictions were excellent. Tables 4 and 5 summarize the analyses of prediction errors for the *RR* and *SS* strains. Recall that the prediction errors were obtained from the halves of the *RR* or *SS* data sets designated for model validation. The prediction errors analysed in Tables 4 and 5 have been standardized (centred at their mean and divided by their standard deviation) in order to separate autocorrelation and normality evaluation from prediction bias evaluation. No significant first-order or second-order autocorrelation was detected in any of the time series in the 'validation' data (Tables 4 and 5). Departure from a normal distribution was detected in just 14 (39%)
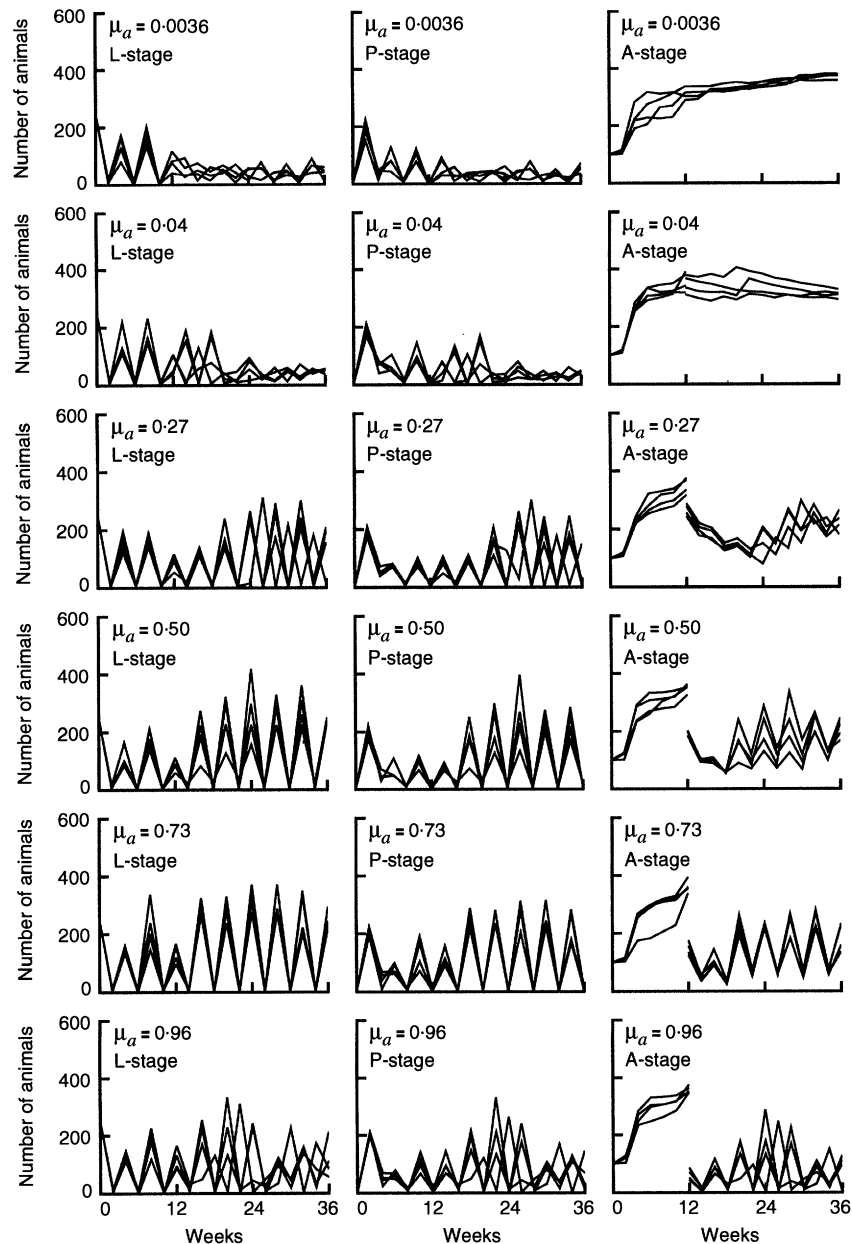
Fig. 4. Transitions in dynamical behaviour are displayed in the time-series data for the individual replicates of the *RR* strain. Top panel: control populations (μ_a unmanipulated). Lower panels: treatment populations (μ_a manipulated).

of the 36 *RR* series and eight (22%) of the *SS* series. Again, a small number of outliers caused these departures. These results compare favourably with the same analyses reported by Dennis *et al.* (1995) for 27 series of the sensitive strain (one first-order autocorrelated series (4%), two second-order autocorrelated series (7%), 10 non-normal series (37%)).

Prediction bias was negligibly small. A prediction bias would be indicated if the prediction errors were centred at a non-zero value. A systematic tendency for the model to underpredict or overpredict would be the cause. Each series of prediction errors was tested for whether or not it arose from a distribution with a mean of zero (*t*-test). Only three of the 36 *RR* strain series showed significantly non-zero means (replicate 1, P_t: $T = -2.46$, $P = 0.03$; replicate 8, L_t:

$T = 2.40$, $P = 0.04$; replicate 11, P_t: $T = 3.07$, $P = 0.01$). Only two of the *SS* series showed significantly non-zero means (replicate 17, A_t: $T = -2.83$, $P = 0.02$; replicate 18, A_t: $T = -3.03$, $P = 0.01$). The prediction biases of the three *RR* series on the original scale represent only about two pupae, 13 larvae, and six pupae, respectively; the prediction biases for the two *SS* series are just three adults and seven adults, respectively.

VISUALIZATION OF THE TIME SERIES:
ESTIMATION AND VALIDATION DATA SETS

The residual analyses suggest that most of the systematic, predictable variability in the data was accounted for by the model skeleton (equations 1–3).
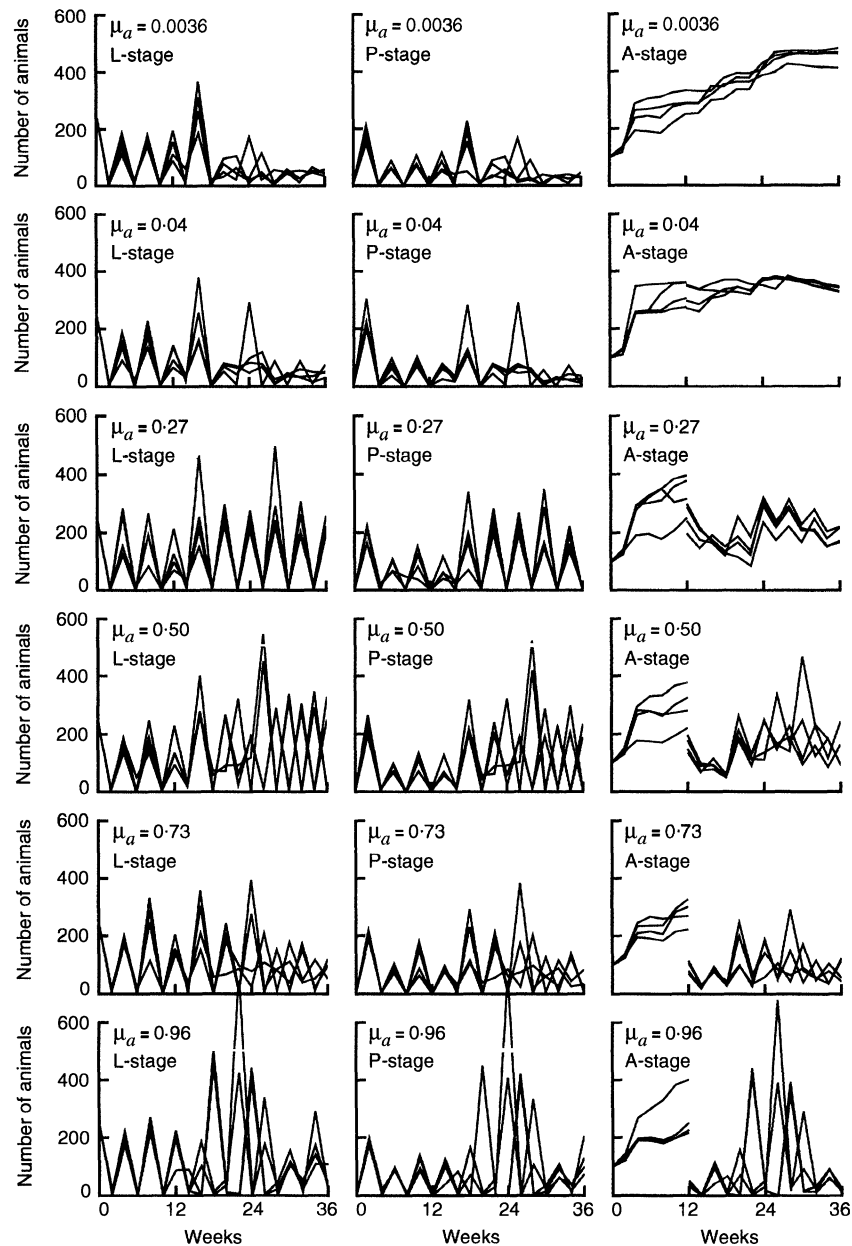
Fig. 5. Transitions in dynamical behaviour are displayed in the time series data for the individual replicates of the *SS* strain. Top panel: control populations (μ_a unmanipulated). Lower panels: treatment populations (μ_a manipulated).

Plots of the data and fitted model support this view. Time series plots for the L-stage, P-stage and A-stage are presented for both the *RR* and *SS* strains in Figs 6–11 and Figs 12–17, respectively, for every population used in the parameter estimation (top six panels) and model validation (bottom six panels). The fitted model is portrayed as one-step predictions (open circles), that is, as the projected value of the state variable at time $t + 1$ (equations 1–3 with ML parameter estimates) given the actual values of the state variables at time t.

As can be seen from the graphs in Figs 6–17, the one-step predictions associated with the 'estimation' data overall are in close agreement across all μ_a treatments for both genetic strains. Stochastic departures from the deterministic one-step forecasts are largest for the L-stage. A typical departure on the original

(nonlogarithmic) scale, as measured by the mean absolute deviation of observed from one-step predicted values, is about 33 L-stage individuals, compared with eight P-stage and six A-stage individuals, for the *RR* strain (*SS*: 43 L-stage, 16 P-stage, 10 A-stage).

The prediction analyses, as discussed in the previous section, confirm that the model skeleton (equations 1–3) accounts for most of the systematic, predictable variability in the data, and that the noise model adequately describes the remaining unpredictable variability. Plots of the 'validation' data and the one-step model predictions illustrate this view (Figs 6–17). The one-step predictions associated with the 'validation' data are in close agreement across all μ_a treatments, for both the *RR* and *SS* strains.

Table 2. Residual analyses for the *RR* strain with the cultures used to estimate the parameters in the model. First- (ρ_1) and second-order (ρ_2) sample autocorrelations and Lin–Mudholkar (Z) test statistic for normality

μ_a	Test statistic	L_t	P_t	A_t	L_t	P_t	A_t
		Replicate 7			Replicate 13		
0·0042	ρ_1	−0·31	0·33	−0·22	0·02	0·09	0·01
(control)	ρ_2	−0·11	0·09	−0·24	0·35	−0·10	0·20
	Z	0·05	1·74	1·60	1·36	2·57*	−1·11
		Replicate 14			Replicate 20		
0·04	ρ_1	−0·04	0·15	−0·02	−0·18	−0·34	0·02
	ρ_2	0·19	0·39	0·59*	0·14	−0·03	−0·16
	Z	−0·02	2·84*	1·31	−0·33	−1·83	−2·83*
		Replicate 3			Replicate 15		
0·27	ρ_1	0·16	0·13	−0·19	0·05	−0·03	−0·16
	ρ_2	0·10	−0·28	0·07	0·50	0·16	0·07
	Z	1·20	−3·46*	4·04*	0·80	0·84	−1·55
		Replicate 4			Replicate 16		
0·50	ρ_1	−0·03	−0·29	0·10	0·39	0·07	0·03
	ρ_2	0·19	−0·25	−0·23	0·34	0·29	−0·33
	Z	1·73	2·48*	−1·50	−0·91	0·53	−1·72
		Replicate 17			Replicate 23		
0·73	ρ_1	−0·01	−0·18	−0·04	−0·01	−0·10	−0·13
	ρ_2	0·11	0·03	0·19	0·05	−0·28	−0·27
	Z	1·22	1·45	−0·72	0·80	−2·73*	−1·84
		Replicate 6			Replicate 12		
0·96	ρ_1	0·01	0·03	0·06	−0·65*	0·04	0·07
	ρ_2	−0·19	−0·12	0·13	0·58*	−0·06	−0·23
	Z	2·11*	2·36*	3·02*	1·01	−2·01*	−2·47*

*ρ_1, ρ_2 significant if $2/\sqrt{q} = 2/\sqrt{12} = 0\cdot577$ is exceeded in absolute value; Z should be a standard normal variate under hypothesis of normality.

Table 3. Residual analyses for the *SS* strain with the cultures used to estimate the parameters in the model. First- (ρ_1) and second-order (ρ_2) sample autocorrelations and Lin–Mudholkar (Z) test statistic for normality

μ_a	Test statistic	L_t	P_t	A_t	L_t	P_t	A_t
		Replicate 7			Replicate 19		
0·0036	ρ_1	−0·14	−0·44	−0·30	−0·31	−0·03	0·32
(control)	ρ_2	−0·29	0·05	−0·17	0·05	−0·46	−0·44
	Z	−1·73	0·01	−2·03*	0·31	1·23	−1·67
		Replicate 8			Replicate 14		
0·04	ρ_1	−0·04	−0·27	−0·02	0·24	0·24	0·11
	ρ_2	−0·35	−0·25	−0·66*	−0·09	0·01	−0·43
	Z	−0·95	0·26	−0·42	−0·76	−0·48	−1·94
		Replicate 9			Replicate 15		
0·27	ρ_1	−0·25	−0·13	0·09	−0·38	0·15	0·08
	ρ_2	0·58*	−0·16	−0·01	0·31	−0·09	−0·10
	Z	1·42	1·26	−1·45	2·01*	3·47*	−0·82
		Replicate 4			Replicate 22		
0·50	ρ_1	−0·35	0·35	0·14	−0·29	0·23	0·34
	ρ_2	−0·12	−0·09	0·13	−0·25	−0·18	−0·27
	Z	2·35*	−0·50	−1·64	−0·80	0·40	−2·01*
		Replicate 5			Replicate 23		
0·73	ρ_1	0·21	0·33	−0·10	−0·13	−0·39	−0·28
	ρ_2	−0·11	0·04	−0·01	0·04	−0·12	0·18
	Z	−0·67	0·25	0·79	0·95	1·36	−0·37
		Replicate 12			Replicate 24		
0·96	ρ_1	−0·14	0·28	−0·01	−0·39	0·07	0·04
	ρ_2	−0·18	−0·47	−0·32	−0·003	0·13	0·14
	Z	0·71	1·84	1·09	−1·16	−2·27*	0·89

*ρ_1, ρ_2 significant if $2/\sqrt{q} = 2/\sqrt{12} = 0\cdot577$ is exceeded in absolute value; Z should be a standard normal variate under hypothesis of normality.

Table 4. Prediction error analyses for the *RR* strain with the cultures used to validate the LPA model. First- (ρ_1) and second-order (ρ_2) sample autocorrelations and Lin–Mudholkar (Z) test statistic for normality

μ_a	Test statistic	L_t	P_t	A_t	L_t	P_t	A_t
		Replicate 1			Replicate 19		
0·0042	ρ_1	0·08	0·11	−0·44	−0·16	0·05	−0·13
(control)	ρ_2	−0·12	0·03	−0·13	−0·49	−0·31	−0·10
	Z	0·23	0·96	−1·67	0·52	−0·42	−1·60
		Replicate 2			Replicate 8		
0·04	ρ_1	−0·23	−0·09	0·05	0·20	0·10	−0·28
	ρ_2	−0·14	−0·21	−0·38	−0·04	−0·27	−0·27
	Z	0·43	4·14*	−1·42	−0·91	2·84*	2·07*
		Replicate 9			Replicate 21		
0·27	ρ_1	−0·003	−0·04	−0·25	0·11	0·18	−0·34
	ρ_2	0·14	−0·36	0·47	0·54	−0·09	0·46
	Z	1·06	−1·81	−1·57	2·29*	2·18*	−2·24*
		Replicate 10			Replicate 22		
0·50	ρ_1	0·13	−0·27	−0·25	0·01	0·12	−0·57
	ρ_2	0·48	−0·07	0·23	0·22	0·01	0·34
	Z	−0·13	−2·98*	−2·28*	3·29*	−1·18	−1·72
		Replicate 5			Replicate 11		
0·73	ρ_1	−0·01	−0·14	−0·32	−0·04	−0·41	−0·38
	ρ_2	0·37	0·02	0·12	0·25	0·15	0·18
	Z	1·10	−1·70	−2·42*	2·14*	−2·25*	−0·36
		Replicate 18			Replicate 24		
0·96	ρ_1	−0·18	0·29	−0·18	−0·53	0·07	−0·12
	ρ_2	0·18	−0·24	0·01	0·32	−0·26	−0·22
	Z	2·19*	−1·73	−0·96	1·35	2·20*	1·00

*ρ_1, ρ_2 significant if $2/\sqrt{q} = 2/\sqrt{12} = 0.577$ is exceeded in absolute value; Z should be a standard normal variate under hypothesis of normality.

Table 5. Prediction error analyses for the *SS* strain with the cultures used to validate the LPA model. First- (ρ_1) and second-order (ρ_2) sample autocorrelations and Lin–Mudholkar (Z) test statistic for normality

μ_a	Test statistic	L_t	P_t	A_t	L_t	P_t	A_t
		Replicate 1			Replicate 13		
0·0036	ρ_1	0·03	0·06	0·37	−0·13	0·20	0·06
(control)	ρ_2	−0·31	0·30	−0·12	0·11	−0·34	−0·53
	Z	0·81	1·73	−1·70	1·19	−0·97	−1·35
		Replicate 2			Replicate 20		
0·04	ρ_1	0·25	0·41	0·20	−0·34	−0·04	0·17
	ρ_2	0·17	0·25	−0·43	0·13	−0·02	−0·22
	Z	−0·36	0·81	−2·22*	0·36	2·18*	−1·61
		Replicate 3			Replicate 21		
0·27	ρ_1	0·12	0·52	−0·02	−0·08	−0·17	0·004
	ρ_2	0·18	0·08	−0·55	−0·14	−0·25	−0·16
	Z	0·41	0·13	−1·33	−0·23	3·07*	−0·42
		Replicate 10			Replicate 16		
0·50	ρ_1	−0·02	0·09	0·38	0·03	−0·10	−0·01
	ρ_2	−0·43	−0·06	−0·01	−0·20	−0·15	0·15
	Z	−1·13	1·58	−1·86	0·49	−2·74*	−1·25
		Replicate 11			Replicate 17		
0·73	ρ_1	−0·31	0·47	0·15	−0·40	−0·25	−0·12
	ρ_2	0·25	0·24	−0·21	0·11	−0·45	0·04
	Z	−0·11	0·79	0·60	2·03*	2·29*	−0·45
		Replicate 6			Replicate 18		
0·96	ρ_1	−0·16	0·36	−0·18	−0·38	0·37	0·08
	ρ_2	0·18	0·05	0·45	−0·12	−0·13	0·10
	Z	−0·65	0·60	2·59*	1·43	2·01*	1·68

*ρ_1, ρ_2 significant if $2/\sqrt{q} = 2/\sqrt{12} = 0.577$ is exceeded in absolute value; Z should be a standard normal variate under hypothesis of normality.
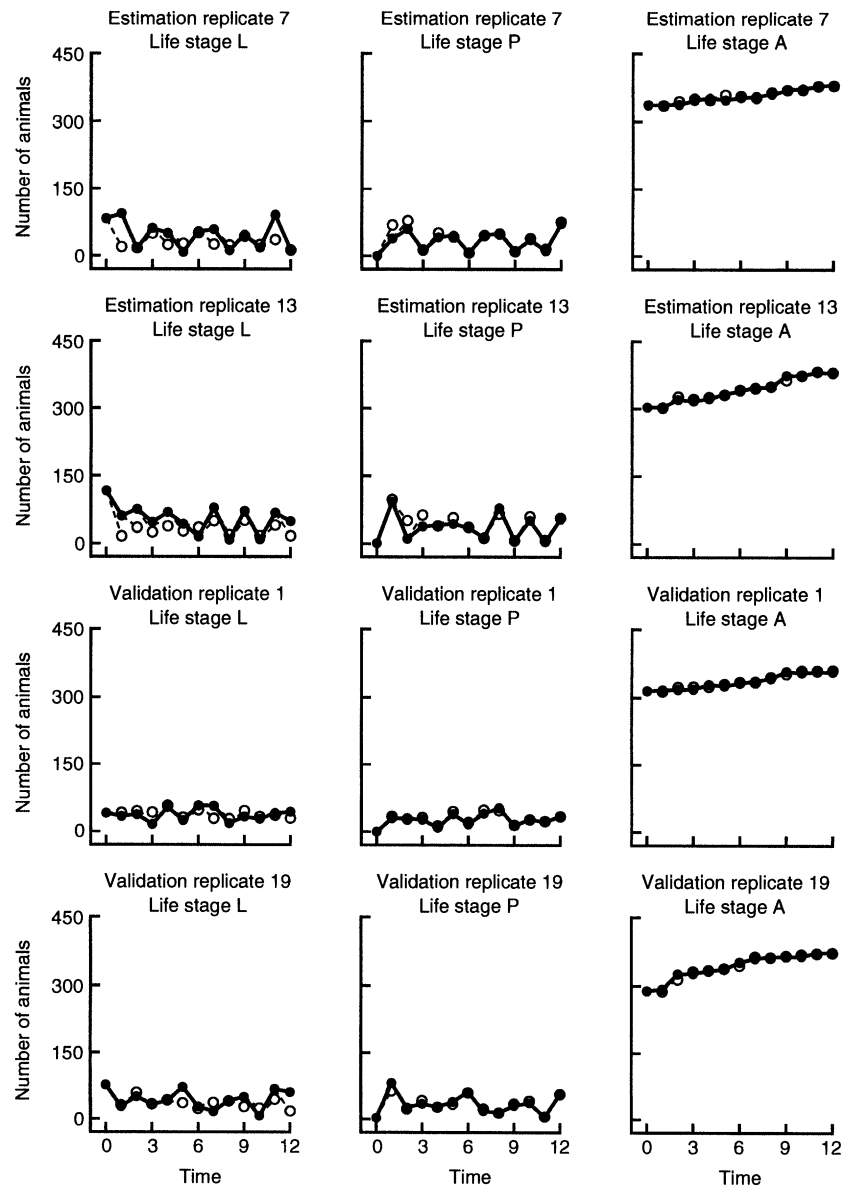
Fig. 6. Census data and one-step predictions for the estimation and validation replicates of the *RR* control treatment.

Discussion

INVARIANT LOOPS

An invariant loop is a mathematical entity best portrayed in phase space (Fig. 18a). It is a closed loop in phase space that is invariant in the sense that trajectories starting at a point on the loop will remain on the loop for all future time. An invariant loop is stable or attracting if any trajectory that starts at a point sufficiently near the loop will tend asymptotically to the loop (in the sense that the distance from the trajectory to the loop tends to zero as time increases without bound). An invariant loop is not a single trajectory but a collection of trajectories, which makes it different from the more familiar attractors such as equilibria and periodic cycles.

Typically, most parameter values causing invariant loop behaviour will produce trajectories having rotational angles around the loop that are irrational

multiples of π, and hence a trajectory on a loop does not ever exactly repeat its initial conditions. Occasionally, windows of parameter values can cause 'period locking,' or true periodic behaviour in which the initial condition on the loop is repeated. Invariant loops represent aperiodic (or period locked) motion, but not chaotic motion. Technical definitions of chaos vary in the nonlinear dynamics literature, but most definitions require some sort of sensitivity to initial conditions (for example, Devaney 1989). The popular quantitative measure of such sensitivity is the Lyapunov exponent (LE). The LE is the exponential rate of change λ in the separation of nearby trajectories (trajectories with small differences in their initial conditions). To an approximation

$$dn_t = dn_0 \, \lambda^t,$$

where n_t is the state of the system (here, for illustration, one-dimensional) at time t, and λ is the LE. If $\lambda > 0$,
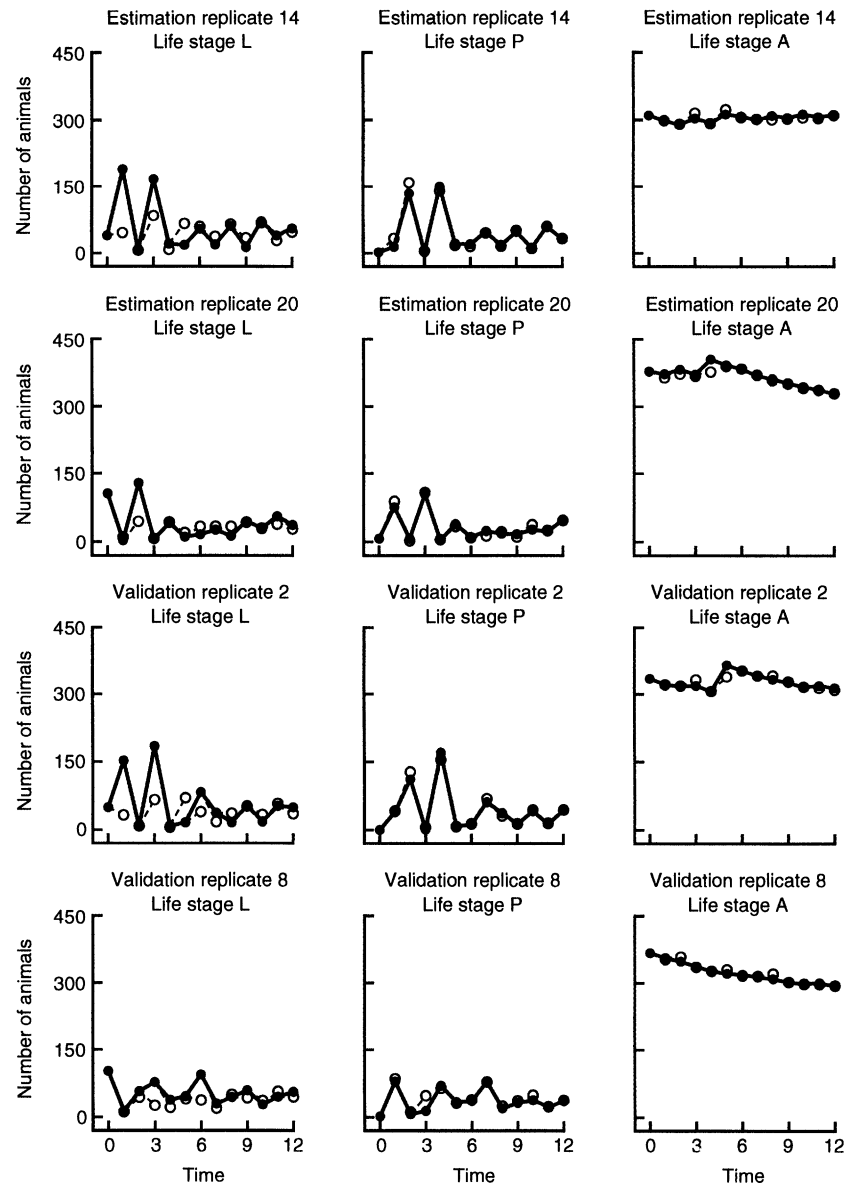
Fig. 7. Census data and one-step predictions for the estimation and validation replicates of the RR $\mu_a = 0.04$ treatment.

a small change in initial conditions represented by dn_0 becomes magnified exponentially through time into a large change dn_t in n_t. For an invariant loop the LE is $\lambda = 0$.

Thus, the invariant loop behaviour displayed by the SS populations at $\mu_a = 0.96$, while aperiodic, is not chaotic. Although we were careful to avoid labelling this behaviour as chaos in our earlier announcement (Costantino *et al.* 1995), the bifurcation diagram (Fig. 3) might be misinterpreted as implying chaos (Rohani & Miramontes 1996).

An invariant loop is a curious object in its own right and is a frequent prediction of nonlinear models. Its documentation in a real biological system is as problematic as the documentation of true chaos. The experimentally induced shifts in dynamic behaviours, we believe, coupled with the results of the model diagnostic and predictive analyses, constitute strong evidence that the fluctuations of the SS populations at $\mu_a = 0.96$ were governed largely by an invariant loop.

Moreover, the evidence strongly suggests that the RR populations at $\mu_a = 0.96$ were influenced by invariant loop-like dynamics. Recall that these RR populations are located near the stability boundary where the stable equilibrium bifurcates into an invariant loop. Near the boundary, trajectories behave similar to trajectories on an invariant loop, except that the amplitude of the cycling is damped inward each time round (Fig. 18b). A trajectory under the RR parameter estimates approaches a stable equilibrium, but only after a long transient period of damped loop-like behaviour.

Invariant loops are important in nonlinear dynamics as a frequent 'route to chaos' (Caswell 1989; Rohani, Miramontes & Hassell 1994; Rohani & Miramontes 1995). The onset of chaos in response to a change in a parameter, in this scenario, is preceded by a regime of invariant loops (aperiodic and period-locking behaviour). A different route to chaos, more familiar to ecologists, is the period-doubling cascade
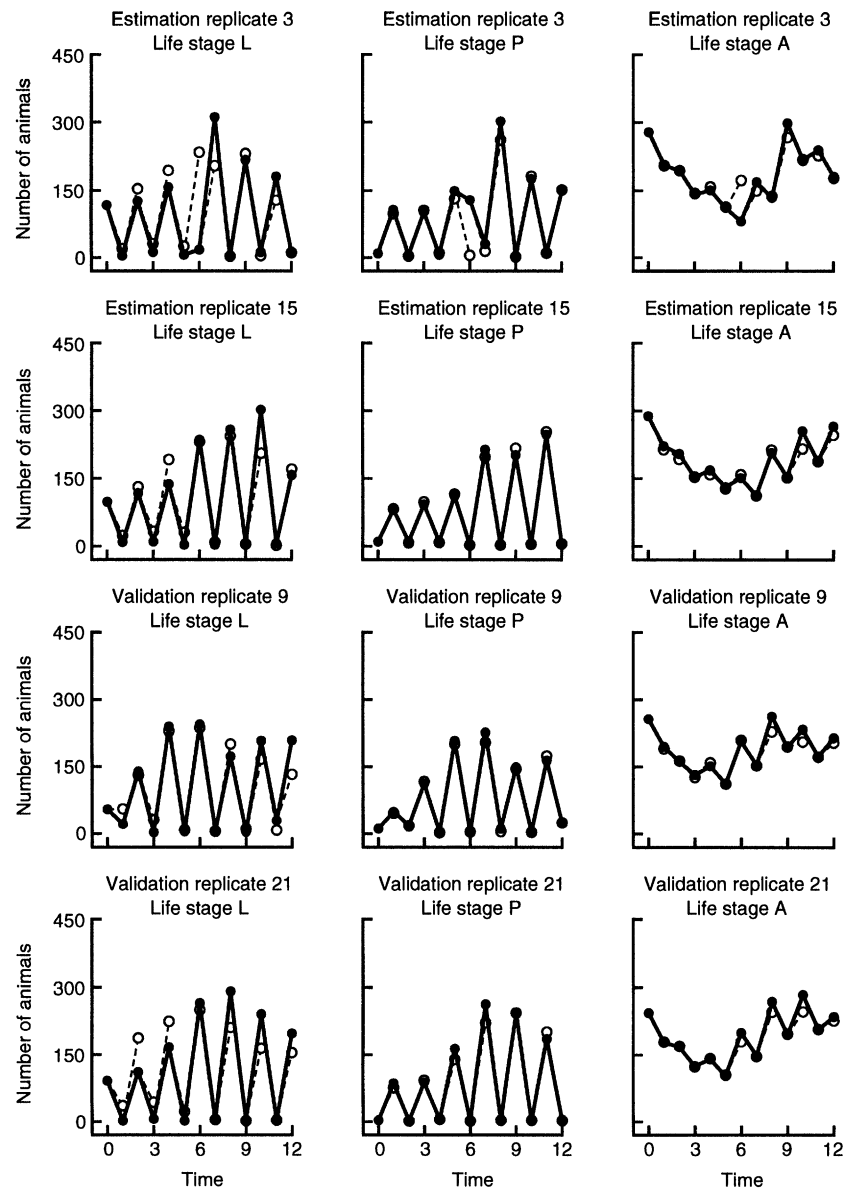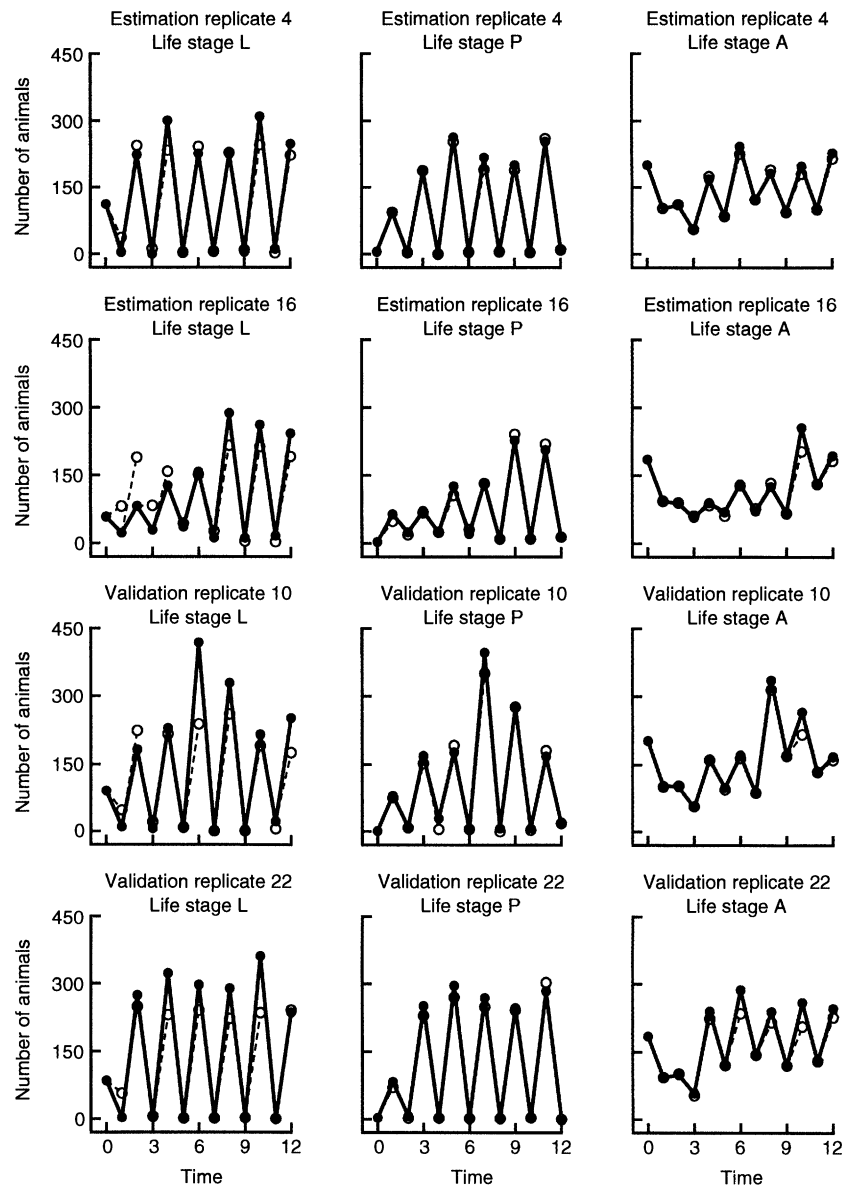
Fig. 8. Census data and one-step predictions for the estimation and validation replicates of the RR $\mu_a = 0.27$ treatment.

exemplified by the logistic map (May 1976). The period-doubling route in fact is observed less frequently in theoretical studies of realistic nonlinear models. The invariant loop behaviour displayed at high μ_a values for the RR and SS parameter estimates points the way to other regions of parameter space where the model displays true chaos (see, Further experiments).

APPROACHES TO TESTING NONLINEAR POPULATION DYNAMICS

There is an enduring uneasiness among ecologists about the role of nonlinear dynamics in our understanding of population fluctuations. 'Applied' mathematical studies of quasi-ecological models have proliferated in the mathematical biology literature, and sorting out the scientific assertions in this literature from purely mathematical results has proved daunting. Ecologists are right to be sceptical about claims

concerning bifurcations, limit cycles and strange attractors in nature. Mathematical ecology studies have too often made oversimplified or unsubstantiated assumptions (Strong 1986a,b). Population models were often proposed without explicit guidelines about how to connect such models to data (Dennis *et al.* 1995). Convincing examples in which a nonlinear population model can be considered reliable knowledge about a real population system are distressingly scarce. Thus, arguments that chaos is prevalent in ecological systems based on the prevalence of chaos in ecological models (see Hastings *et al.* 1993 for a review) have not, in general, found a receptive audience among data-orientated ecologists.

A more intriguing approach to testing nonlinear population dynamics focuses on analysing time series observations of population abundances (reviewed by Hastings *et al.* 1993). The analyses involve using non- or semi-parametric statistical techniques to estimate

Fig. 9. Census data and one-step predictions for the estimation and validation replicates of the RR $\mu_a = 0.50$ treatment.

the map (skeleton) that produced the data. Such analyses have indicated the presence of stable points, stable cycles, and even chaos, in various population systems (Ellner & Turchin 1995). However, the time series in these analyses came from observational studies. Also, the biological mechanisms driving the population fluctuations were hypothesized only, and not included explicitly in the models used to analyse the data. Consequently, these types of analyses are suggestive of an important role for nonlinear dynamics in population fluctuations, but are intrinsically limited in the types of conclusions that can be drawn.

Several recent investigations have attempted to fit or describe natural populations with nonlinear, low-dimensional mechanistic models (Olsen & Schaffer 1990; Grenfell *et al.* 1992; Bolker & Grenfell 1993; Hanski *et al.* 1993; Carpenter, Cottingham & Stow 1994; Hanski & Korpimaki 1995). A growing sub-area of related research is concerned with statistical

methods for fitting such models to time series data (Carpenter *et al.* 1994; Dennis *et al.* 1995; Pascual & Kareiva 1996). For situations in which the main biological interactions are well known, this approach has potential for showcasing nonlinear population models as practical data analysis tools. Important details regarding the forms of the models, though, such as whether a predation function should be prey-dependent or ratio-dependent, can remain non-identifiable, especially when there are sampling errors in the data (see Carpenter *et al.* 1994; Pascual & Kareiva 1996). Predictions of chaos and other dynamical behaviours, such as those issued by Hanski *et al.* (1993) for boreal rodents, can hinge on fine details of model structure (Sturis & Knudsen 1996). The observational nature of the data is also a limitation of this type of approach; system manipulations may be necessary to distinguish between contending models (Carpenter *et al.* 1994).
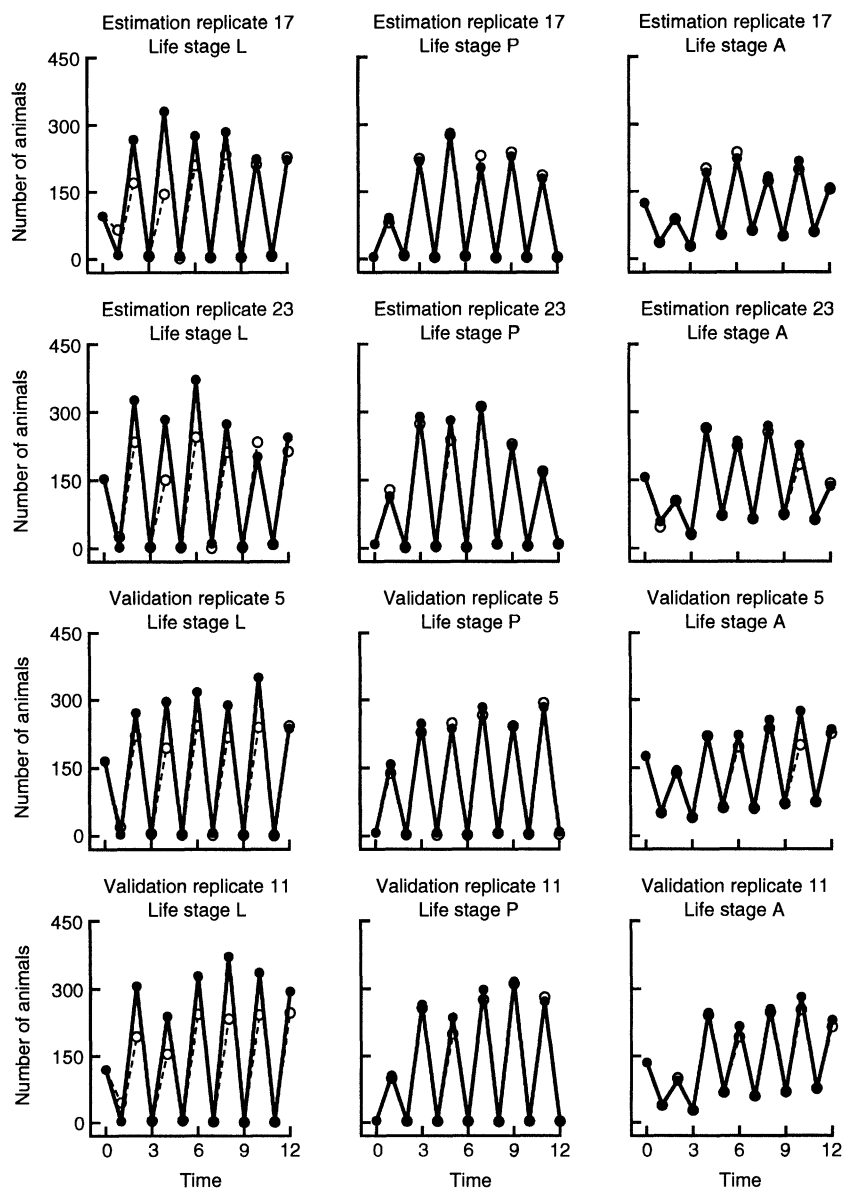
Fig. 10. Census data and one-step predictions for the estimation and validation replicates of the $RR\ \mu_a = 0.73$ treatment.

Our study was not aimed at documenting chaos, *per se*. Rather, our study was aimed at the broader question of whether or not the modelling methods of nonlinear dynamics could provide an accurate quantitative description of a biological population. Our goal was to find out how well a biologically based model would perform under ecologically idealized conditions. Our particular model was a stage-structured model believed to include the main interactions influencing the population fluctuations. The model was developed by us earlier (Dennis *et al.* 1995) and based on almost 70 years of flour beetle research by numerous investigators (see Costantino & Desharnais 1991 for a review). The experimental system was easily censused, replicated, and manipulated. Under such conditions, if nonlinear dynamics is to be taken seriously in population biology, we would expect the model to make detailed, accurate predictions.

Hutchinson's oft-repeated argument that lab-

oratory populations are simply analogue computers set up to solve model equations (for instance Colinveaux 1973; Hutchinson 1978) was either glib or excessively optimistic about mathematical population models. Laboratory systems are beguilingly complex, and sorting out the essential regulating mechanisms can consume whole careers (Park *et al.* 1970, p. 183). While laboratory microcosms cannot substitute for manipulative field experiments (Carpenter 1996), the isolation of treatment factors possible in the laboratory has been useful for testing basic ecological concepts and has historically complemented field results (Ives *et al.* 1996). Certainly, success stories connecting mathematical modelling and laboratory experiments have been few and far between. As a result, Kareiva (1989) issued an emphatic call for more bottle experiments (see also Godfray & Blythe 1990), and for better, more direct couplings of mathematical models and data.
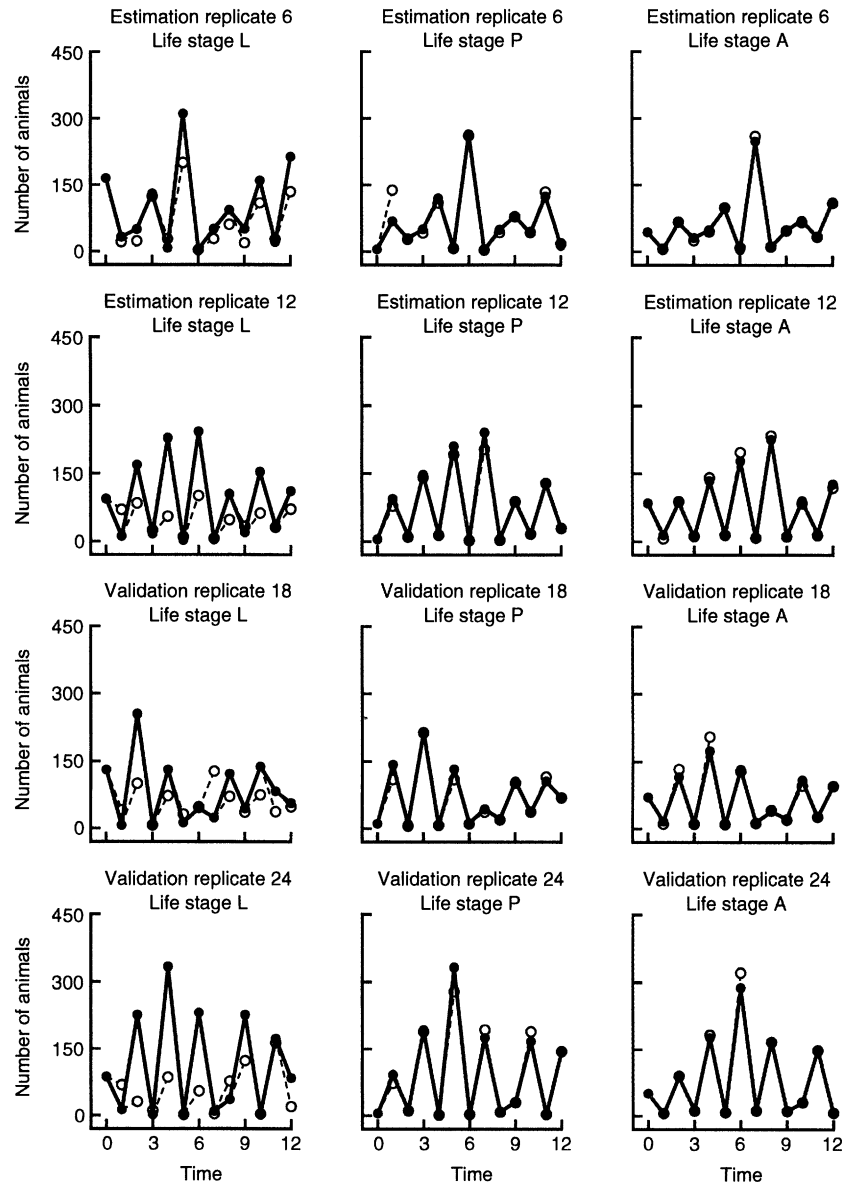
Fig. 11. Census data and one-step predictions for the estimation and validation replicates of the *RR* $\mu_a = 0.96$ treatment.

FURTHER EXPERIMENTS

The LPA model (equations 1–3) makes some intriguing predictions about dynamic behaviours for other regions of parameter space. Although the present experiment did not produce 'chaos in a bottle,' the prospect of true chaos is certainly predicted for other parameter values; for instance, the dynamical behaviour at the adult mortality value of $\mu_a = 0.96$ in the present experiment was at (*SS* strain) or near (*RR* strain) invariant loop behaviour. Because invariant loops are a common 'route to chaos' (Caswell 1989; Rohani *et al.* 1994; Rohani & Miramontes 1995), it makes sense to hunt for chaos in nearby regions of parameter space.

Suppose the adult-on-pupae cannibalism parameter, c_{pa}, were changed, with all other parameters remaining at the estimated values, and with $\mu_a = 0.96$. Model simulations reveal a striking series

of predicted transitions in dynamic behaviour as the value of c_{pa} changes. Figure 19 displays the predicted bifurcation diagram for the L-stage abundances of the *RR* strain. As c_{pa} increases, a transition from stable equilibria to invariant loop behaviour (aperiodic) occurs, followed by transitions to period-locking (periodic behaviour), and chaos. At around $c_{pa} = 0.43$, the chaos region is predicted to break down suddenly into a region of stable three-cycles which extends to $c_{pa} = 1.00$. However, embedded within this region of stable three-cycles is a period doubling/chaos attractor; this region of multiple attractors extends from $c_{pa} = 0.56$ to $c_{pa} = 0.70$. An experimental study designed to evaluate these predictions has recently been completed (Costantino *et al.* 1997).

Other predictions of intriguing nonlinear behaviours in the LPA model have emerged; we mention two.
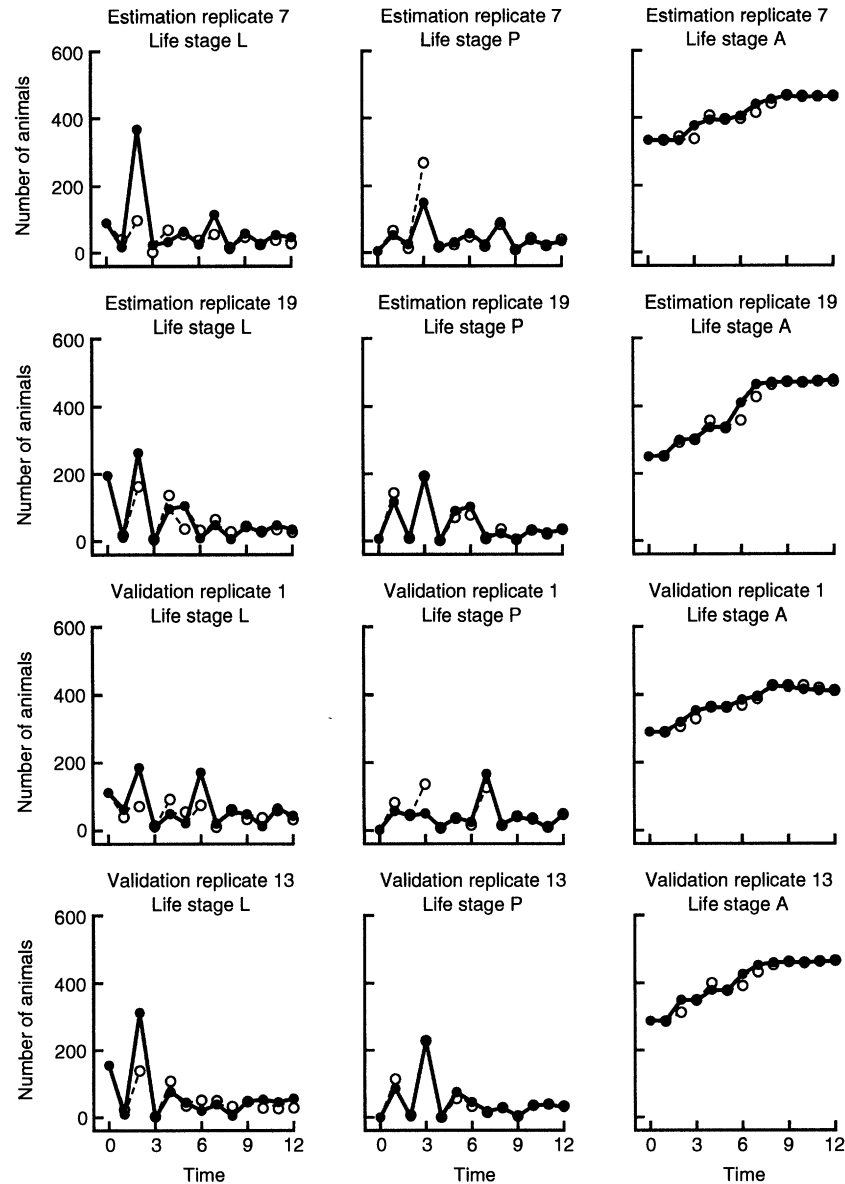
First, the exponential nonlinearities in the LPA

Fig. 12. Census data and one-step predictions for the estimation and validation replicates of the *SS* control treatment.

model describe the basic mechanism of search-and-encounter cannibalism. The exponential terms can be reparameterized to show explicitly the volume of flour in the culture container (the volume is currently 'absorbed' in the parameters c_{el}, c_{ea}, and c_{pa}). With flour volume represented, the effects of time-varying habitat sizes can be studied analytically and simulated. Multiple attractors, and the 'Jillson effect' (increase of overall population abundance in periodically fluctuating habitats; Jillson 1980) are among the behaviours predicted for *Tribolium* populations in containers with periodically alternating volumes of flour (Henson & Cushing 1997; R.F. Costantino *et al.*, unpublished).

Second, when the point equilibrium of the LPA equations (1–3) is unstable, it resides on a low-dimensional stable manifold. Trajectories that start near the stable manifold (or are shoved near by stochastic noise) execute a 'fly-by' (approach and near-miss) of the

unstable equilibrium en route to the stable attractor (Cushing *et al.* 1996, unpublished). Thus, because the stochastic noise eventually perturbs the population away from the stable attractor and into the region of influence of the stable manifold, a long trajectory is predicted to show an occasional transient fly-by of the unstable equilibrium.

For both of the above situations, straightforward laboratory experiments should reveal the predicted behaviours. Such experiments would constitute further strong tests of the LPA model. Indeed, much even remains to be discovered about the mathematical properties of the model itself.

IMPLICATIONS FOR APPLIED ECOLOGY

The experimental results should give pause to equilibrium-based theories of harvesting biological resources. The concept of 'sustained yield,' whether
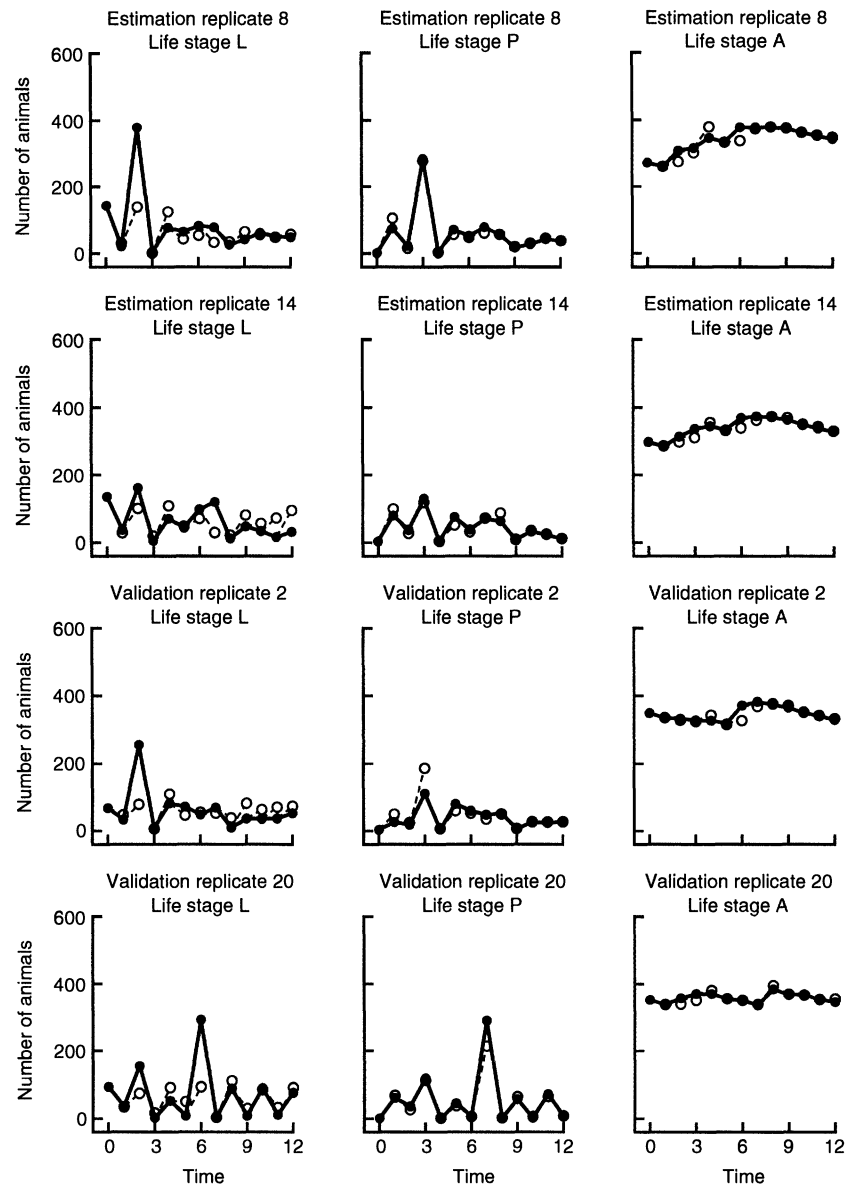
Fig. 13. Census data and one-step predictions for the estimation and validation replicates of the SS $\mu_a = 0.04$ treatment.

maximum, optimum or otherwise, is based on a point equilibrium attractor (Clark 1976). According to these theories, the point equilibrium of the resource responds smoothly to moderate changes in the harvest rate, with the possible exception that the equilibrium could collapse at high harvest rates due to depensation or Allee effects (Clark 1976; Dennis 1989). Management sets a harvest rate for whatever objective, then waits for the population system to settle down and give forth an equilibrium yield for whatever time period.

However, if the system has nonlinear feedbacks, the equilibrium is not necessarily a point. The attractor could be an n-cycle, a loop or a strange attractor; the system could even have multiple attractors.

The LPA model (equations 1–3) resembles a stage-structured Ricker model, albeit with some unusual complexities in the density-dependent feedbacks. The Ricker model is routinely used in fisheries management to describe fish recruitment and set sustained

yield policies (Newman 1993). Many fish species are in fact cannibalistic (adults on eggs or juveniles), and the Ricker exponential nonlinearity is frequently an appropriate mechanistic as well as purely descriptive model. Even a simple one-stage Ricker model has the potential for displaying a variety of stable attractors (May 1976).

In our experiment, the adult mortality parameter μ_a can be regarded as a harvest rate. In response to experimentally set harvest rates, the system displayed not only point equilibria, but two-cycles and invariant loops as well. In the SS strain at $\mu_a = 0.96$, the 'sustained yield' is aperiodic; population sizes (and yields) under this regime vary widely. With the inescapable stochastic noise present, the trajectories would occasionally be influenced by the stable manifold in the system. The enduring cyclic or aperiodic behaviour, coupled with occasional fly-bys of a point equilibrium, would appear quirky to managers without a
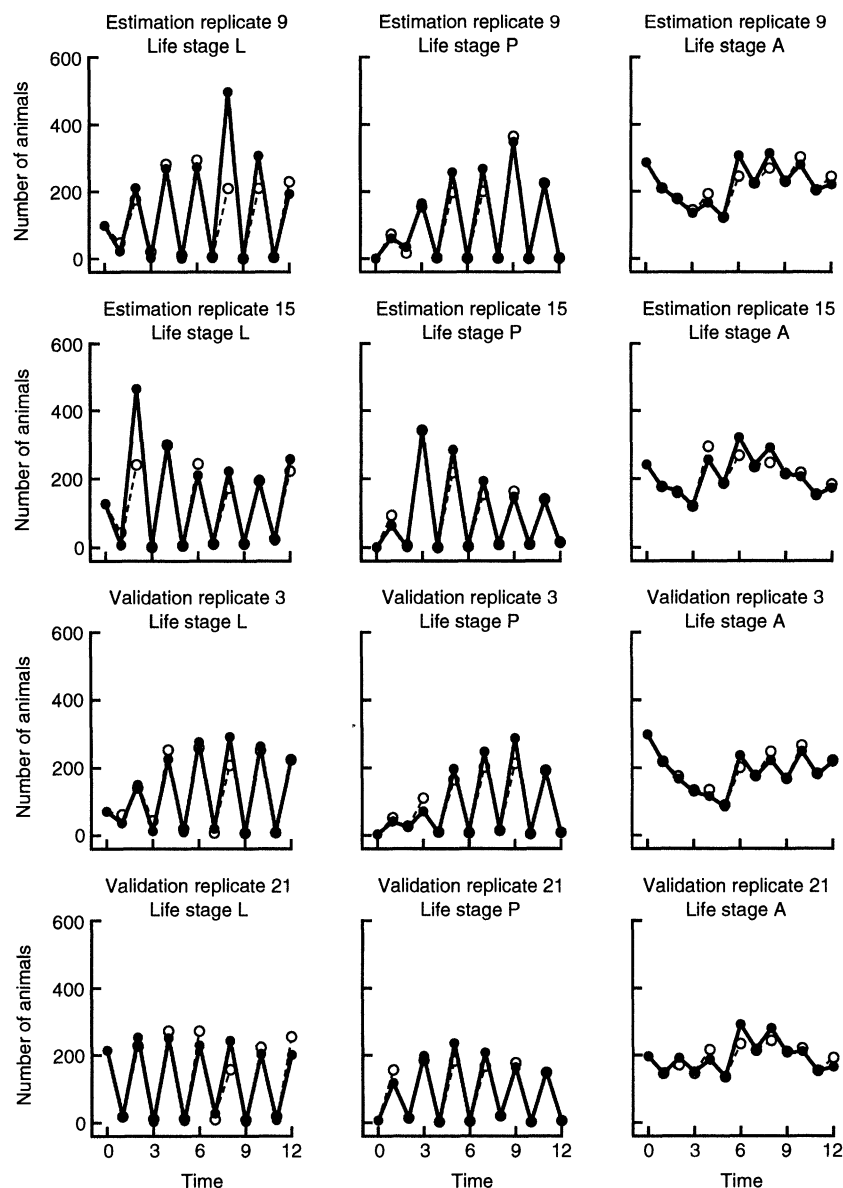
Fig. 14. Census data and one-step predictions for the estimation and validation replicates of the SS $\mu_a = 0.27$ treatment.

detailed understanding of the biological interactions in the system.

The experiment also suggests a cautious approach to pest management (Kareiva 1995). The adult mortality treatments can be likened to pest reduction measures of varying severities. The nonlinear feedbacks in the system, however, here caused the reduction efforts to fail. What were stable equilibria in various treatments became unstable equilibria (stable cycles or loops) upon the increase of μ_a. Wide oscillations ensued in which the upswings in adult population sizes were higher than the stable equilibrium sizes. That nature's nonlinear feedbacks might cause pest reduction efforts to backfire has been a theme of pest dynamics theory for many years (for instance, Allen 1989; Logan 1989).

CONCLUDING REMARKS

In our view, one of the key predictions emerging from nonlinear ecological modelling is not that populations are likely to be chaotic *per se*, but rather that populations will undergo transitions among behaviours associated with different attractors in response to changing conditions. We demonstrated that fluctuations of a stage-structured population system could be explained and closely forecasted by a low-dimensional nonlinear model. In response to our experimental manipulations of a control parameter, the system displayed the bifurcations and attractor behaviours predicted by the model. Careful attention to the statistical connections between model and data was a feature of our work. We believe the approach and results reported here point the way to a heightened level of relevance of nonlinear mathematics in population biology.
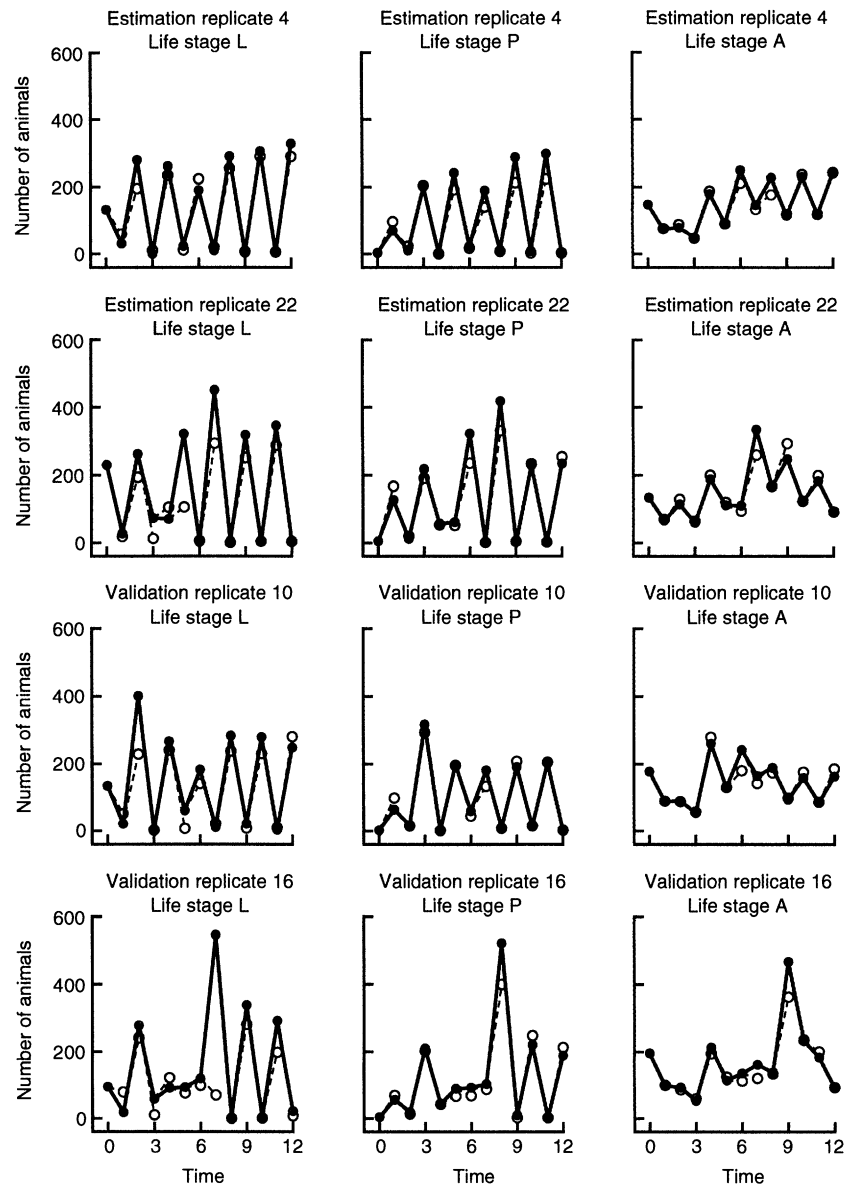
Fig. 15. Census data and one-step predictions for the estimation and validation replicates of the SS $\mu_a = 0.50$ treatment.
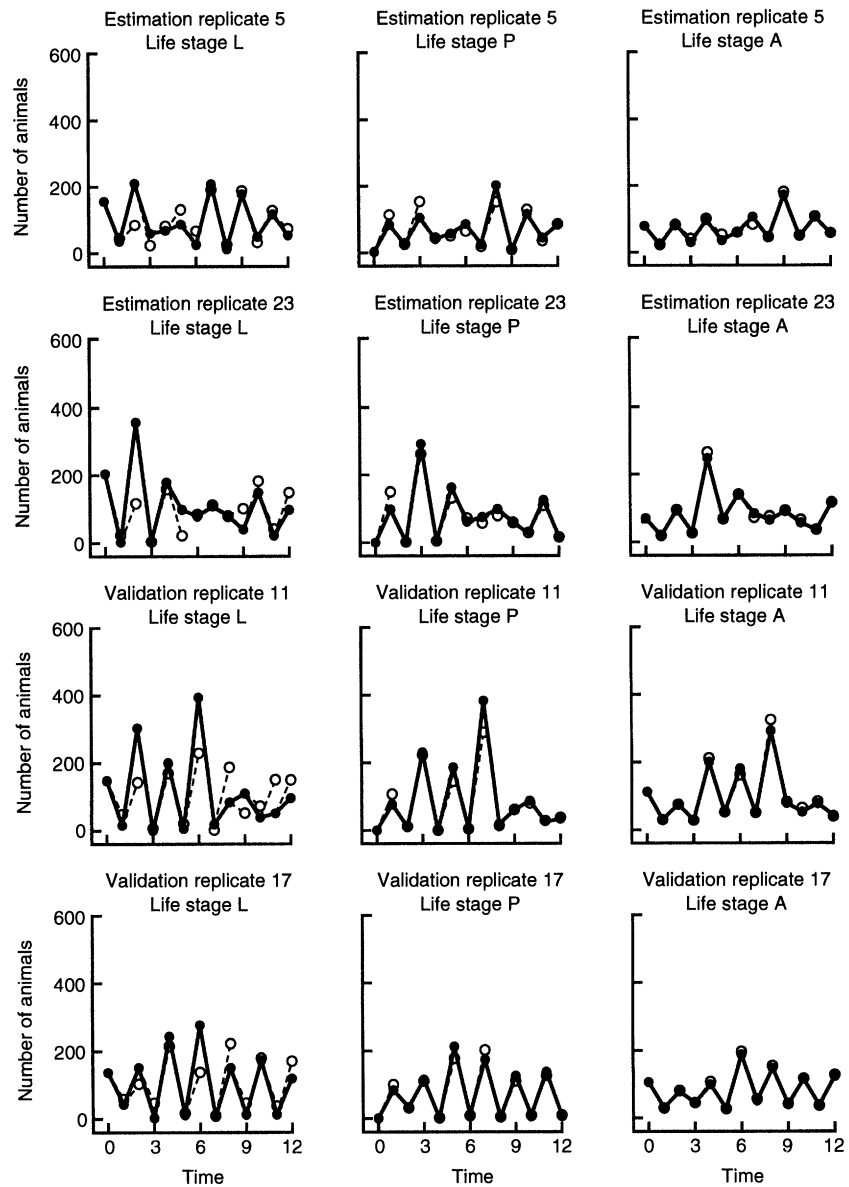
Fig. 16. Census data and one-step predictions for the estimation and validation replicates of the SS $\mu_a = 0.73$ treatment.
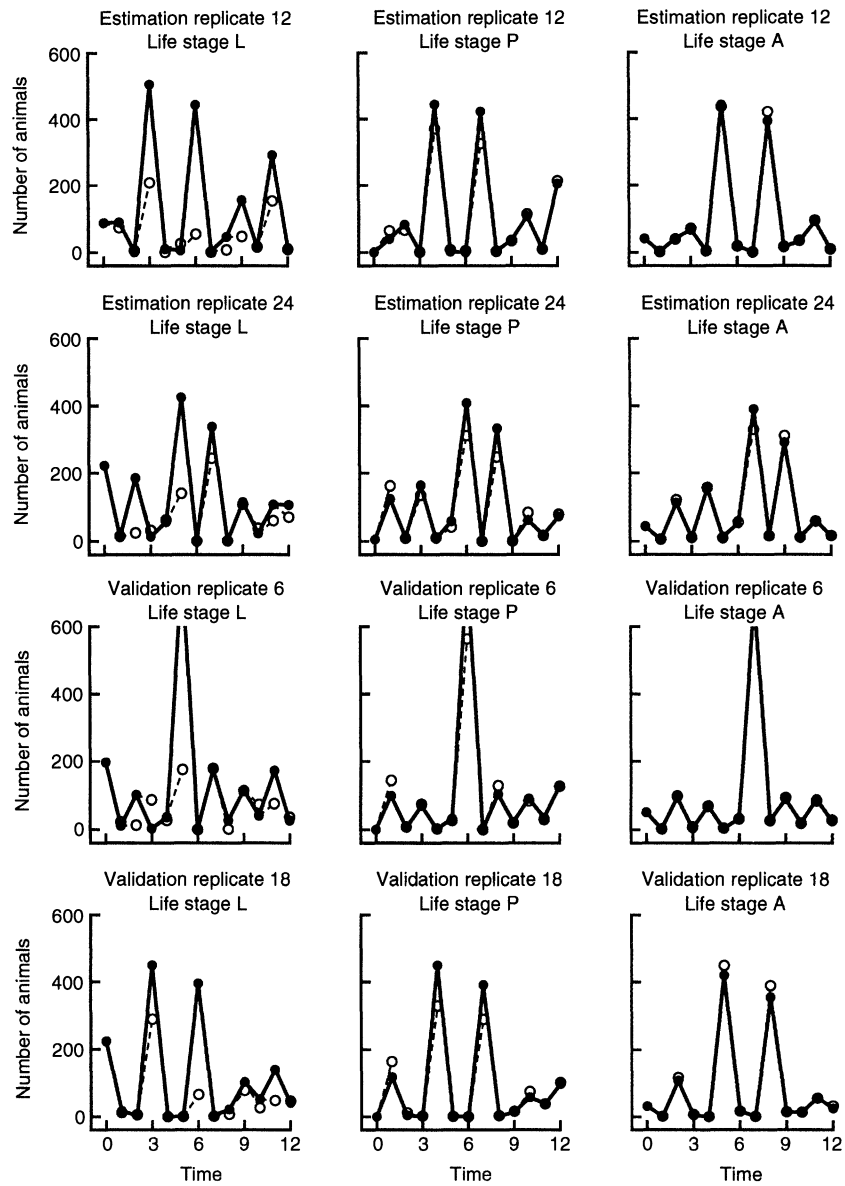
Fig. 17. Census data and one-step predictions for the estimation and validation replicates of the *SS* $\mu_a = 0.96$ treatment.
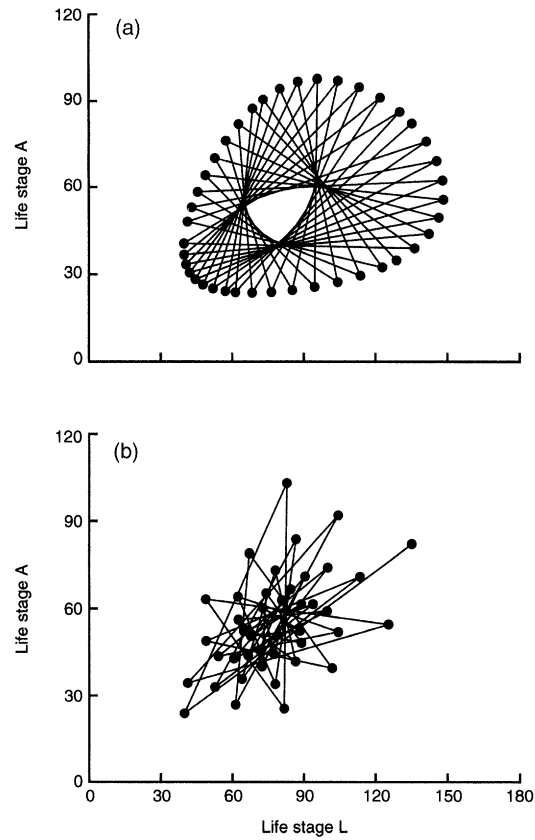
Fig. 18. Phase space graphs shown projected onto the L-stage, A-stage plane. (a) An invariant loop. (b) Invariant loop-like transient dynamics that eventually approach a stable equilibrium.
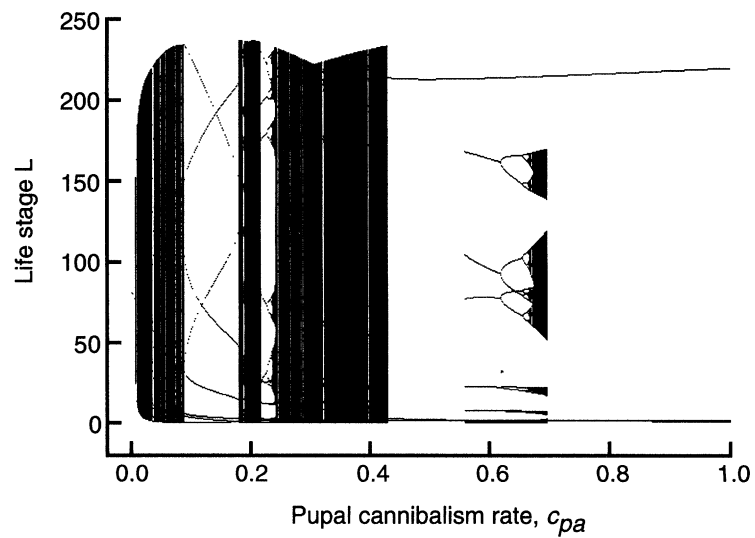

Fig. 19. The predicted bifurcation diagram for the L-stage abundances of the *RR* strain with $\mu_a = 0.96$ and the other parameters as given in Table 1.

References

Allen, J.C. (1989) Are natural enemy populations chaotic? *Estimation and Analysis of Insect Populations* (L. McDonald, B. Manly, J. Lockwood, & J. Logan eds), pp. 190–205. Springer-Verlag, Berlin.

Ascioti, F.A., Betrami, E., Carroll, T.O., & Wirick, C. (1993) Is there chaos in plankton dynamics? *Journal of Plankton Research*, **15**, 603–617.

Bartlett, M.S. (1990) Chance or chaos? (with discussion.) *Journal of the Royal Statistical Society A*, **52**, 321–347.

Berryman, A.A. (1991) Can economic forces cause ecological chaos? The case of the northern California Dungeness crab fishery. *Oikos*, **62**, 106–109.

Berryman, A.A. & Millstein, J.A. (1989) Are ecological systems chaotic and if not, why not? *Trends in Ecology & Evolution*, **4**, 26–28.

Bolker, B.M. & Grenfell, B.T. (1993) Chaos and biological complexity in measles dynamics. *Proceedings of the Royal Society of London B*, **251**, 75–81.

Carpenter, S.R. (1996) Microcosm experiments have limited relevance for community and ecosystem ecology. *Ecology*, **77**, 677–680.

Carpenter, S.R., Cottingham, K.L. & Stow, C.A. (1994) Fitting predator–prey models to time series with observation errors. *Ecology*, **75**, 1254–1264.

Caswell, H. (1989) *Matrix Population Models*. Sinauer Associates, Sunderland, MA.

Clark, C.W. (1976) *Mathematical Bioeconomics: The Optimal Management of Renewable Resources*. John Wiley, New York.

Colinveaux, P. (1973) *Introduction to Ecology*. John Wiley, New York.

Costantino, R.F. & Desharnais, R.A. (1991) *Population Dynamics and the* Tribolium *Model: Genetics and Demography*. Springer-Verlag, New York.

Costantino, R.F., Cushing, J.M., Dennis, B. & Desharnais, R.A. (1995) Experimentally induced transitions in the dynamic behavior of insect populations. *Nature*, **375**, 227–230.

Costantino, R.F., Desharnais, R.A., Cushing, J.M. & Dennis, B. (1997) Chaotic dynamics in an insect population. *Science*, **275**, 389–391.

Cushing, J.M. (1995) Systems of difference equations and structured population dynamics. *Proceedings of the First International Conference on Difference Equations* (eds S. N. Elaydi, J. R. Graef, G. Ladas, & A. C. Peterson), pp. 190–205. Gordon and Breach Publishers, Amsterdam.

Cushing, J.M., & Yicang, Z. (1994) The net reproductive value and stability in structured population models. *Natural Resource Modeling*, **8**, 1–37.

Cushing. J.M., Dennis, B., Desharnais, R.A. & Costantino, R.F. (1996) An interdisciplanary approach to understanding nonlinear ecological dynamics. *Ecological Modelling*, **92**, 111–119.

Dennis, B. (1989) Allee effects: population growth, critical density, and the chance of extinction. *Natural Resource Modeling*, **3**, 481–538.

Dennis, B., Desharnais, R.A., Cushing, J.M. & Costantino, R.F. (1995) Nonlinear demographic dynamics: mathematical models, statistical methods, and biological experiments. *Ecological Monographs*, **65**, 261–281.

Desharnais, R.A. & Costantino, R.F. (1980) Genetic analysis of a population of Tribolium VII. Stability: response to genetic and demographic perturbations. *Canadian Journal of Genetics and Cytology*, **22**, 577–589.

Devaney, R.L. (1989) *Introduction to Chaotic Dynamical Systems*, 2nd edn. Benjamin-Cummings, Menlo Park, California.

Ellner, S. & Turchin, P. (1995) Chaos in a noisy world: new methods and evidence from time-series analysis. *American Naturalist*, **145**, 343–375.

Godfray, H.C.J. & Blythe, S.P. (1990) Complex dynamics in multispecies communities, *Philosophical Transactions of the Royal Society of London B*, **330**, 221–233.

Godfray, H.C.J. & Grenfell, B.T. (1993) The continuing quest for chaos. *Trends in Ecology & Evolution*, **8**, 43–44.

Grasman, J. & van Straten, G (eds) (1994) *Predictability and Nonlinear Modelling in Natural Sciences and Economics*. Kluwer Academic Publishers, Dordrecht.

Grenfell, B.J., Price, O.F., Albon, S.D. & Clutton-Brock, T.H. (1992) Overcompensation and population cycles in an ungulate. *Nature*, **355**, 823–826.

Hanski, I. & Korpimaki, E. (1995) Microtine rodent dynamics in northern Europe: parameterized models for the predator–prey interaction. *Ecology*, **76**, 840–850.

Hanski, I., Turchin, P., Korpimaki, E. & Henttonen, H. (1993) Population oscillations of boreal rodents: regulation by mustelid predators leads to chaos. *Nature*, **364**, 232–235.

Hassell, M.P., Comins, H.N., & May, R.M. (1991) Spatial structure and chaos in insect population dynamics. *Nature*, **353**, 255–258.

Hastings, A., Hom, C.L., Ellner, S., Turchin, P., & Godfray, H.C.J. (1993) Chaos in ecology: Is mother nature a strange attractor? *Annual Review of Ecology and Systematics*, **24**, 1–33.

Henson, S.M. & Cushing, J.M. (1997) The effect of periodic habitat fluctuations on a nonlinear insect population model. *Journal of Mathematical Biology* (in press).

Hutchinson, G.E. (1978) *An Introduction to Population Ecology*. Yale University Press, New Haven.

Ives, A.R., Foufopoulos, J., Klopfer, D., Krug, J.L. & Palmer, T.M. (1996) Bottle or big-scale studies: how do we do ecology? *Ecology*, **77**, 681–685.

Jillson, D. (1980) Insect populations respond to fluctuating environments. *Nature*, **288**, 699–700.

Kareiva, P. (1989) Renewing the dialogue between theory and experiments in population ecology. *Perspectives in Ecological Theory* (J. Roughgarden, R. M. May & S. A. Levin eds), pp. 68–88. Princeton University Press, New Jersey.

Kareiva, P. (1995) Predicting and producing chaos. *Nature*, **375**, 189–190.

Kuang, Y., & Cushing, J.M. (1995) Global stability in a nonlinear difference-delay equation model of flour beetle population growth. *Journal of Difference Equations & Applications*, **2**, 31–37.

Logan, J.A. (1989) Derivation and analysis of composite models for insect populations. *Estimation and Analysis of Insect Populations* (L. McDonald, B. Manly, J. Lockwood, & J. Logan eds), pp. 278–288. Springer-Verlag, Berlin.

Logan, J.A. & Allen, J.C. (1992) Nonlinear dynamics and chaos in insect populations. *Annual Review of Entomology*, **37**, 455–477.

Logan, J.A. & Hain, F.P (eds) (1991) *Chaos and Insect Ecology*. Virginia Experiment Station Information Series 91–3, Virginia Polytechnic Institute and State University, Blacksburg.

May, R.M. (1974) Biological populations with non-overlapping generations: stable points, stable cycles and chaos. *Science*, **186**, 645–647.

May, R.M (ed.) (1976) *Theoretical Ecology: Principles and Applications*. W.B. Saunders, Philadelphia.

May, R.M. (1986) When two and two do not make four: nonlinear phenomena in ecology. *Proceedings of the Royal Society of London B*, **228**, 241–266.

May, R.M. (1987) Chaos and the dynamics of biological populations. *Proceedings of the Royal Society of London A*, **413**, 27–44.

Newman, E.I. (1993) *Applied Ecology*. Blackwell Scientific Publications, Oxford.

Olsen, L.F., & Schaffer, W.M. (1990) Chaos vs. noisy periodicity: alternative hypotheses for childhood epidemics. *Science*, **249**, 499–504.

Park, T., Nathanson, M., Ziegler, J.R. & Mertz, D.B. (1970) Cannibalism of pupae by mixed-species populations of adult *Tribolium*. *Physiological Zoology*, **43**, 166–184.

Pascual, M.A. & Kareiva, P. (1996) Predicting the outcome of competition using experimental data: Maximum likelihood and Bayesian approaches. *Ecology*, **77**, 337–349.

Poole, R. (1989a) Is it chaos, or is it just noise? *Science*, **243**, 25–28.

Poole, R. (1989b) Ecologists flirt with chaos? *Science*, **243**, 310–313.

Press, W.H., Teukolsky, S.A., Vetterling, W.T. & Flannery, B.P. (1992) *Numerical Recipes: the Art of Scientific Computing*, 2nd edn. Cambridge University Press, Cambridge.

Renshaw, E. (1994) Chaos in biometry. *IMA Journal of Mathematics Applied in Medicine & Biology*, **11**, 17–44.

Rohani, P. & Miramontes, O. (1995) Immigration and persistence of chaos in population models. *Journal of Theoretical Biology*, **175**, 203–206.

Rohani, P. & Miramontes, O. (1996) Chaos or quasiperiodicity in laboratory insect populations? *Journal of Animal Ecology*, **65**, 847–849.

Rohani, P., Miramontes, O. & Hassell, M.P. (1994) Quasiperiodicity and chaos in population models. *Proceedings of the Royal Society of London B*, **258**, 17–22.

Scheuring, I. & Janosi, I.M. (1996) When two and two make four: a structured population without chaos. *Journal of Theoretical Biology*, **178**, 89–97.

Strong, D.R. (1986a) Population theory and understanding pest outbreaks. *Ecological Theory and Integrated Pest Management* (M. Kogan ed.), pp. 37–58. John Wiley & Sons, New York.

Strong, D.R. (1986b) Density vague population change. *Trends in Ecology & Evolution*, **1**, 39–42.

Sturis, J. & Knudsen, C. (1996) Modelling seasonal predator–prey interactions. *Journal of Theoretical Biology*, **178**, 99–103.

Tilman, D. & Wedin, D. (1991) Oscillations and chaos in the dynamics of a perennial grass. *Nature*, **353**, 653–655.

Tong, H. (1990) *Nonlinear Time Series: a Dynamical Systems Approach*. Oxford University Press, Oxford.

Tong, H. & Smith, R.L (eds) (1992) Royal Statistical Society meeting on chaos. *Journal of the Royal Statistical Society B*, **54**, 301–474.

Turchin, P. (1993) Chaos and stability in rodent population dynamics: evidence from nonlinear time-series analysis. *Oikos*, **68**, 167–172.

Turchin, P. & Taylor, A.D. (1992) Complex dynamics in ecological time series. *Ecology*, **73**, 289–305.

Wilson, J.A., Acheson, J.M., Metcalfe, M., & Kleban, P. (1994) Chaos, complexity and community management of fisheries. *Marine Policy*, **18**, 291–305.